ADVANCED CONTROL FOR FLOATING OFFSHORE WIND TURBINES

DOCTORAL THESIS

BY

JOANNES OLONDRIZ ERDOZAIN

Leioa, 2019

ADVANCED CONTROL FOR FLOATING OFFSHORE WIND TURBINES

Doctoral thesis submitted for the degree of Doctor, accepted by the Electricity and Electronics Department of the Faculty of Science and Technology of the University of the Basque Country UPV/EHU in partnership with Ikerlan Technology Research Centre, Control and Monitoring area.

Principal co-supervisors:

Prof. Dr. Santiago Alonso Quesada (University of the Basque Country UPV/EHU)

Dr. Carlos Calleja Elcoro (Ikerlan Technology Research Centre)

Advisor:

Prof. Dr. Josu Jugo García (University of the Basque Country UPV/EHU)

Leioa, 2019

Universidad del País Vasco Euskal Herriko Unibertsitatea

NAZIOARTEKO BIKAINTASUN CAMPUSA
CAMPUS DE EXCELENCIA INTERNACIONAL

AUTORIZACION DEL/LA DIRECTOR/A DE TESIS

PARA SU PRESENTACION

Dr/a. _____con N.I.F._____

como Director/a de la Tesis Doctoral: _____

_____

_____

realizada en el Programa de Doctorado _____

_____

por el Doctorando Don/ña. _____ ,

autorizo la presentación de la citada Tesis Doctoral, dado que reúne las condiciones necesarias para su defensa.

En _____a _____de _____de _____

EL/LA DIRECTOR/A DE LA TESIS

Fdo.: _____

Universidad del País Vasco Euskal Herriko Unibertsitatea

NAZIOARTEKO BIKAINTASUN CAMPUSA
CAMPUS DE EXCELENCIA INTERNACIONAL

AUTORIZACION DEL/LA DIRECTOR/A DE TESIS

PARA SU PRESENTACION

Dr/a. _____con N.I.F._____

como Director/a de la Tesis Doctoral: _____

_____

_____

realizada en el Programa de Doctorado _____

_____

por el Doctorando Don/ña. _____ ,

autorizo la presentación de la citada Tesis Doctoral, dado que reúne las condiciones necesarias para su defensa.

En _____a _____de _____de _____

EL/LA DIRECTOR/A DE LA TESIS

Fdo.: _____

Universidad del País Vasco Euskal Herriko Unibertsitatea

NAZIOARTEKO BIKAINTASUN CAMPUSA
CAMPUS DE EXCELENCIA INTERNACIONAL

AUTORIZACION DEL TUTOR/A DE TESIS

PARA SU PRESENTACION

Dr/a. _____

_____

como Tutor/a de la Tesis Doctoral: _____

_____

_____

realizada en el Programa de Doctorado _____

_____

por el Doctorando Don/ña. _____ ,

y dirigida por el Dr./a _____

autorizo la presentación de la citada Tesis Doctoral, dado que reúne las condiciones necesarias para su defensa.

En _____a _____de _____de _____

EL/LA TUTOR/A DE LA TESIS

Fdo.: _____

AUTORIZACIÓN DEL DEPARTAMENTO

El Consejo del Departamento de _____

_____

en reunión celebrada el día ___ de _____ de _____ ha acordado dar la conformidad a la admisión a trámite de presentación de la Tesis Doctoral titulada: _____

_____
_____
_____

dirigida por el/la Dr/a. _____

---

y presentada por Don/ña. _____

ante este Departamento.

En _____ a _____ de _____ de _____

VºBº DIRECTOR/A DEL DEPARTAMENTO

SECRETARIO/A DEL DEPARTAMENTO

Fdo.: _____

Fdo.: _____

Universidad del País Vasco | Euskal Herriko Unibertsitatea

NAZIOARTEKO BIKAINTASUN CAMPUSA
CAMPUS DE EXCELENCIA INTERNACIONAL

AUTORIZACIÓN DE LA COMISIÓN ACADÉMICA DEL PROGRAMA DE DOCTORADO

La Comisión Académica del Programa de Doctorado en _____

_____

en reunión celebrada el día ____ de _____ de 20___, ha acordado dar la conformidad a la presentación de la Tesis Doctoral titulada: _____

_____

_____

dirigida por el/la Dr/a. _____

_____

y presentada por Don/Dña. _____

adscrito o adscrita al Departamento _____

_____

En _____a _____de _____de _____

EL/LA RESPONSABLE DEL PROGRAMA DE DOCTORADO

Fdo.: _____

Universidad del País Vasco | Euskal Herriko Unibertsitatea

NAZIOARTEKO BIKAINTASUN CAMPUSA
CAMPUS DE EXCELENCIA INTERNACIONAL

ACTA DE GRADO DE DOCTOR O DOCTORA
ACTA DE DEFENSA DE TESIS DOCTORAL

DOCTORANDO/A DON/DÑA. _____

TITULO DE LA TESIS: _____

_____

_____

El Tribunal designado por la Comisión de Postgrado de la UPV/EHU para calificar la Tesis Doctoral arriba indicada y reunido en el día de la fecha, una vez efectuada la defensa por el/la doctorando/a y contestadas las objeciones y/o sugerencias que se le han formulado, ha otorgado por_____la calificación de:

unanimidad ó mayoría

SOBRESALIENTE / NOTABLE / APROBADO / NO APTO

Idioma/s de defensa (en caso de más de un idioma, especificar porcentaje defendido en cada idioma):

Castellano _____

Euskera _____

Otros Idiomas (especificar cuál/cuales y porcentaje) _____

En _____a _____de _____de _____

EL/LA PRESIDENTE/A, EL/LA SECRETARIO/A,

Fdo.: Fdo.:

Dr/a: _____ Dr/a: _____

VOCAL 1º, VOCAL 2º, VOCAL 3º,

Fdo.: Fdo.: Fdo.:

Dr/a: _____Dr/a:_____Dr/a:_____

EL/LA DOCTORANDO/A,

Fdo.: _____

ADVANCED CONTROL FOR FLOATING OFFSHORE WIND TURBINES

Author: Joannes Olondriz Erdozain

List of publications:

- Paper A: Olondriz J., Elorza I., Trojaola I., Pujana A., Landaluze J. *On the effects of basic platform design characteristics on floating offshore wind turbine control and their mitigation.* J. Phys. Conf. Ser. (Torque **2016**), 753.
- Paper B: Olondriz J., Elorza I., Calleja C., Jugo J., Pujana A. *Platform negative damping, blade root and tower base bending moment reductions with an advanced control technique.* WindEurope Conference & Exhibition **2017**.
- Paper C: Olondriz J., Elorza I., Jugo J., Alonso-Quesada S., Pujana-Arrese A. *An Advanced Control Technique for Floating Offshore Wind Turbines Based on More Compact Barge Platforms.* Energies **2018**, 11, 1187.
- Paper D: Olondriz J. Jugo J., Elorza I., Alonso-Quesada S., Pujana-Arrese A. *Alternative linearisation methodology for aero-elastic Floating Offshore Wind Turbine non-linear models.* J. Phys. Conf. Ser. (Torque **2018**), 1037.
- Paper E: Olondriz J., Wei Y., Jugo J., Lemmer F., Elorza I., Alonso-Quesada S., Pujana-Arrese A. *Using Multiple Fidelity Numerical Models For Floating Offshore Wind Turbine Advanced Control Design.* Energies **2018**, 11, 2484.
- Paper F: Olondriz J., Jugo J., Elorza I., Alonso-Quesada S., Pujana-Arrese A. *A Blade Load Feedback Control for Floating Offshore Wind Turbines.* WindEurope Conference & Exhibition **2019**.
- Paper G: Olondriz J., Jugo J., Elorza I., Alonso-Quesada S., Pujana-Arrese A. *A Feedback Control Loop Optimisation Methodology for Floating Offshore Wind Turbines.* Energies (unpublished).

Gehien maite ditudan pertsonei, zuek
gabe hau ez litzatekeelako posible izango

Abstract

Wind energy is becoming the real green energy alternative to the conventional fossil fuel sources, as the increment of the new wind farm projects worldwide demonstrates. The offshore wind presents many advantages compared to its onshore counterpart, but the current bottom-fixed technology is limited by the water depth since the supporting structures can only be installed in shallow water coastal areas. Therefore, a solution to overcome this limitation has been developed by mounting the wind turbines on floating structures, i.e. the Floating Offshore Wind Turbines.

Early studies of Floating Offshore Wind Turbines have shown that control plays an important role for the dynamic behaviour of the system due to the possible platform negative damping effect. Therefore, several control techniques have been proposed in the last years in order to avoid such a negative effect and improve the performance of the Floating Offshore Wind turbines.

In this thesis, an advanced control technique has been designed and tuned to improve the overall performance of Floating Offshore Wind Turbines in terms of power regulation and global mechanical loadings, as well as to reduce the impact of the waves in the floating platform motion. Two platform concepts have been studied with more detail, (1) the ITI Energy's barge concept with 5-MW wind turbine and (2) the 10-MW wind turbine on a TripleSpar concept. The first model has been chosen because its basic and economic design, the fabrication and installation advantages, and the challenges posed to the turbine control system by less stable and more compact platforms. Furthermore, the

relationship between the fundamental platform dimensions and the operating performance, specially in terms of challenges posed to the turbine control system, is investigated with more compact barge models. Besides, the second model has been chosen to prove the scalability of the designed advanced control technique in a higher power rated wind turbine mounted on a hydrodynamically more stable platform. Furthermore, an optimisation methodology to automatically tune the advanced controller has been developed based on the Damage Equivalent Loads results, improving the manually tuned controller outcomes.

Two alternative linearisation strategies for Floating Offshore Wind Turbines are proposed. The first one uses the generator torque trimming while the second applies the chirp signal methodology. The generator torque trimmed linear models show acceptable results, while the chirp signal methodology delivers the highest fidelity results respect to the identification of the system modes.

For the hydrodynamic analysis of floating platforms, the open source code NEMOH has been proposed to obtain the hydrodynamic matrices required for the simulation code FAST. The obtained results have been compared with those obtained with WAMIT code, validating the approach from the method development point of view.

The obtained results suggest a significant effectiveness of the designed advanced control technique for reducing the mechanical loads suffered in tower and blades while improving the wind turbine performance, contributing to achieve a cost effective solution for the Floating Offshore Wind Turbine technology.

Acknowledgements

I would like to thanks *Ikerlan Technology Research Centre* for supporting and giving me the opportunity of developing my PhD studies and, to my mates of the Control and Monitoring area who have help me in minor or major extent in the development of this work.

My deep gratitude is addressed to Josu Jugo and Santi Alonso from Basque Country University UPV/EHU for providing me with excellent advice, great support and never-ending encouragement.

Further, I would like to thank my colleagues at the Stuttgart Wind Energy institute for giving me the opportunity to make the enjoyable, unforgettable and successful PhD stay.

And finally and most importantly, I owe my deepest gratitude to my friends, couple and family for showing an interest in my work, their help in forgetting about it for some time and, their understanding if this was not possible.

Eskerrik asko,

Joannes O.

Contents

List of Figures

List of Tables

Glossary

APS	Aerodynamic Platform Stabiliser
BEM	Boundary Element Method
BPF	Band-Pass Filter
BVP	Boundary-Value Problem
CAE	Computer-aided Aeroelastic Engineering
CM	Centre of Mass
CPC	Collective Pitch Control
D	Derivative
DAC	Disturbance-Accomodating Control
DEL	Damage Equivalent Loads
DLC	Design Load Case
DNV-GL	Det Norske Veritas and Germanischer Lloyd
DOF	Degree Of Freedom
DTU	Denmark Technical University
FAST	Fatigue, Aerodynamics, Structures, and Turbulence
FFT	Fast Fourier Transformation
FOWT	Floating Offshore Wind Turbines
GE	General Electric
GK	Gain-Correction Factor
GM	Metacentric Height
GS	Gain-Scheduling
GWEC	Global Wind Energy Council
H_∞	H-infinity

HAWT	Horizontal-Axis Wind Turbine
HMPC	Hybrid Model Predictive Control
HSS	High Speed Shaft
I	Integral
IEA	International Energy Agency
IEC	International Electrotechnical Commision
IPC	Individual Pitch Control
IQR	Inter-Quartile Range
JONSWAP	Joint North Sea Wave Project
LCOE	Levelised Cost Of Energy
LIDAR	Light Detection and Ranging
LPF	Low-Pass Filter
LPV	Linear Parameter-Varaying
LQR	Linear Quadratic Regulator
MBS	Multi-Body System
MIMO	Multiple-Input Multiple-Output
MPC	Model Predictive Control
NAME	Naval Architecture and Marine Engineering
NMPZ	Non-Minimum Phase Zeros
NREL	National Renewable Energy Laboratory
P	Proportional
PD	Proportional and Derivative
PI	Proportional and Integral
PID	Proportional, Integral and Derivative
PSD	Power Spectral Density
PZO	Pole and Zero Optimisation
RBF	Radial Basis Function
SF	State-Feedback
SISO	Single-Input Single-Output
SLOW	Simplified Low-Order Wind turbine
SS	State Space
STD	Standard Deviation
SWE	Stuttgart Wind Energy

SWL	Still Water Level
TLP	Tension Leg Platform
TPES	Total Primary Energy Supply
TRL	Technology Readiness Level
TSR	Tip Speed Ratio
VPPC	Variable Power Pitch Control
WAMIT	Wave Analysis at MIT
WR	Wave Rejection

Symbols

a	= control loop switching weighting factor
A	= amplitude of a sinusoidal wave
A_{ij}	= (i,j) component of the impulsive hydrodynamic-added-mass matrix
A_s	= the area of the section
β	= incident-wave propagation heading direction
B_{ij}	= (i,j) component of the hydrodynamic-damping matrix
c	= tower-platform interface
C_p	= power coefficient
$C_{p_{max}}$	= maximum power coefficient
ζ_φ	= damping ratio of the response associated with the equation of motion for the rotor-speed error
$\ddot{\underline{q}}$	= set of second time derivatives of the system DOF
$\dot{\underline{q}}$	= set of first derivatives of the system DOF
e	= error value between a desired set-point and a measured feedback
f_0	= initial frequency (sweep-sine signal)
f_1	= final frequency (sweep-sine signal)
$\underline{f}_k$	= non-linear force vector
$f(t)$	= instantaneous frequency
G	= gear-box relation
γ	= propagation decay constant
h	= barge internal structure density

H_s	= significant wave height
$I_{Drivetrain}$	= drivetrain inertia cast to the low-speed shaft
j	= when not used as a subscript, this is the imaginary number, $\sqrt{-1}$
J	= partial cost term
J_T	= current cost function
J_{T0}	= initial cost function
k	= k^{th} degree of freedom
K	= controller gain (PI controller)
K_c	= control loop switching static gain
K_{limit}	= controller gain limit to ensure system stability
K_i	= integral gain
K_p	= proportional gain
λ	= (or TSR) ratio between the tangential speed of the blade tip and the current wind speed
λ_{opt}	= optimum TSR
M	= mass matrix
M_{xyT}	= tower-base-roll to -pitch bending moment
M_g	= generator torque
M_{xB}	= blade-root-edgewise bending moment
M_{xT}	= tower-base-roll bending moment
M_{yB}	= blade-root-flapwise bending moment
M_{yT}	= tower-base-pitch bending moment
N_{Gear}	= high-speed to low-speed bear-box ratio
ω	= angular frequency
Ω_g	= generator speed
Ω_g^*	= reference generator speed
Ω_r	= rotor speed
Ω_{r0}	= rated rotor speed
$\omega_{\varphi n}$	= natural frequency of the response associated with the equation of motion for the rotor-speed error
ω_{xn}	= natural frequency of the response associated with the equation of motion of the platform-pitch in terms of the translation of the hub

ϕ	= phase angle
P_n	= nominal mechanical power
$\partial P/\partial\theta$	= sensitivity of the aerodynamic power to the rotor-collective blade-pitch angle
$\underline{q}$	= set of system DOF
R	= radious of the rotor
ρ	= air density
σ	= change factor (PZO method)
t	= time
T	= time interval (sweep-sine signal)
t_c	= barge shell thickness
θ	= blade-pitch angle
θ^*	= blade-pitch angle reference
θ_{APS}	= blade-pitch angle of the APS feedback loop
θ_K	= rotor-collective blade-pitch at which the pitch sensitivity has doubled from its value at the rated operating point
θ_{PI}	= blade-pitch angle of the PI feedback loop
θ_{yP}	= platform-pitch angle
θ_{xP}	= platform-roll angle
θ_{WR}	= blade-pitch angle of the WR feedback loop
T_i	= integrator time constant (PI controller)
T_p	= peak spectral period
$\underline{u}$	= vector of the control inputs
$\underline{u_d}$	= vector of the input disturbances
V_w	= wind speed
W	= weight of the partial cost term
X_i	= i^{th} component of the frequency- and direction-dependent complex incident-wave-excitation force on the support platform per unit wave amplitude
xOz	= orthogonal axes x-z plane

CHAPTER

1

Introduction

This chapter aims to provide the context of the Ph.D. research done on the advanced control of floating offshore wind turbines. An introduction to offshore wind energy is presented first, continuing with the motivation which has encouraged the development of this research, as well as its objectives and scope. An outline of the thesis is given at the end of this chapter.

1.1 Offshore Wind Energy

Greenhouse gas emissions and the exhaustion of fossil resources have increased the urgency of concerns about global warming as well as the necessity for developing renewable energy production alternatives worldwide. Since the early 70's, and thanks to supportive governmental policies, some sources of renewable energy, such as solar, hydro and wind electricity, have been gradually taking on an important role in the world's Total Primary Energy Supply (TPES). Concretely, renewable energies have kept their rank as the third largest contributor to global electricity production during the recent period. They accounted for 23.8% of world generation, after coal (27.9%) and gas (27.7%), but ahead of nuclear (18.0%) and oil (2.0%), according to the International Energy Agency (IEA) [1].

Among renewable energy technologies, the wind energy sector has experienced a remarkable growth in the last decade. Currently, Asia is the largest wind energy contributor in the world, followed by the EU, the US, and South America. The global amount of accumulative wind energy capacity was $539,123$ MW in 2017, according to the Global Wind Energy Council (GWEC)[1]. The vast majority of wind energy is installed onshore; however, the expansion of the wind energy production to offshore emplacements has contributed to this growth. After the first offshore wind farm was installed in Denmark in 1991, called Vindeby, an exponential increase has been seen in the cumulative offshore wind energy capacity worldwide [2], as can be seen in the left side of Figure 1.1. The largest contributor is the UK, amounting to 36.3% of the total installed offshore wind capacity, followed by Germany with 28.5%, China with 14.8%, and so on.

Offshore wind energy production, i.e. the generation of electricity by means of wind turbines installed at sea some miles offshore, has several advantages over conventional onshore wind energy production: (1) the areas with the best wind quality for wind energy production can be reached, so the offshore wind power generation is higher per amount of installed capacity; (2) it solves the lack of available terrain for new onshore wind farm emplacements, reducing the visual and noise pollution for nearby neighbourhoods; and (3) it has a lesser environmental impact on the forests as well as on wildlife [3].

[1] https://gwec.net/global-figures/graphs/

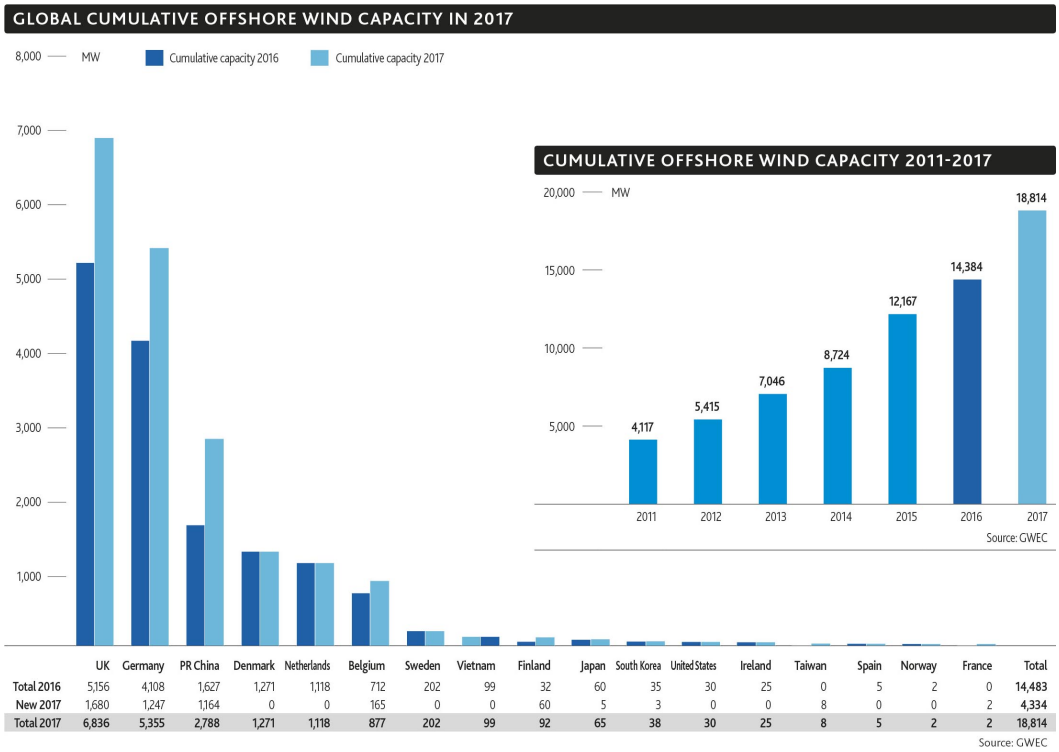

	UK	Germany	PR China	Denmark	Netherlands	Belgium	Sweden	Vietnam	Finland	Japan	South Korea	United States	Ireland	Taiwan	Spain	Norway	France	Total
Total 2016	5,156	4,108	1,627	1,271	1,118	712	202	99	32	60	35	30	25	0	5	2	0	14,483
New 2017	1,680	1,247	1,164	0	0	165	0	0	60	5	3	0	0	8	0	0	2	4,334
Total 2017	6,836	5,355	2,788	1,271	1,118	877	202	99	92	65	38	30	25	8	5	2	2	18,814

Source: GWEC

Figure 1.1: Global offshore wind energy capacity according to GWEC.

The sea remains a vast space where at first sight there seems to be enough space for offshore wind farms. Nevertheless, the current technological solutions for harvesting offshore wind energy, i.e. bottom-fixed wind turbines (gravity base, pilot, jacket, ...) (see Figure 1.2), are designed for areas of shallow water, with depths less than 80–100 m [4]. However, it is becoming progressively less economical and more difficult (or impossible) to install in depths of water of more than 30–40 metres [5][6]. This limitation reduces significantly the available offshore areas worldwide for the installation of bottom-fixed wind turbines. Thus, an alternative solution to overcome this limitation is required, such as mounting the offshore wind turbines onto a floating structure [7], i.e. the Floating Offshore Wind Turbines (FOWT) (see Figure 1.2). This provides the chance to produce electricity in areas of deep water, which is especially desirable for steeply-shelving coastal countries.

The first vision of mounting a large-scale wind turbine on a floating structure was in 1972, by Professor William E. Heronemos at the University of Massachusetts, Amherst (MA, USA). Some publications appeared [8][9] before the idea was

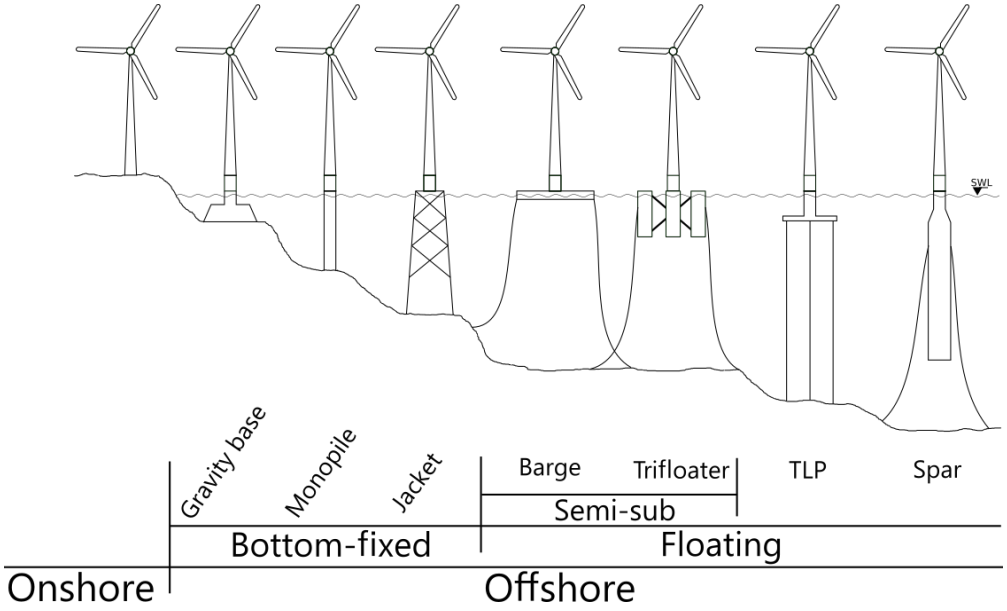

Figure 1.2: Illustrative representation of the main offshore wind turbine concepts.

taken up again in the late 90's by the commercial wind industry, which started carrying out the first research studies and moving the topic to the academic sector. Research in FOWT systems was not carried out until that decade due to the wind market's being focused on developing bottom-fixed wind turbines in shallow water areas. Although several institutions started researching in FOWT, it was not until the year 2007 when the first FOWT prototype was launched into the sea in Italy, named BlueH. This project marked the beginning of a new era for offshore wind energy, with the materialisation of that academic idea. Since then, more than a dozen prototypes have been tested worldwide, most of them in the EU, but also in the US and Japan. Although this technology is in its early development stages, some commercial projects have been carried out. As of 2018, the world's first operational floating wind farm started producing electricity in Scotland. Past, present and near future FOWT projects are analysed in detail in Section 2.2.

1.2 Motivation

At present, bottom-fixed wind turbines are cheaper to build because they use the existing onshore technology for their monopiles and jacket structures. The current FOWT projects, however, require an individualised structure fabrication, mounting, deployment and installation, including special boats and cranes for the installation and towing, increasing all of them the final Levelised Cost Of Energy (LCOE) [10]. Once the floating technology reaches a more developed technological stage and the floating platforms go into series production, mass production can reduce their fabrication cost. According to experts, the FOWT technology will take between 10 and 15 years to mature and be able to compete with the other currently available sources of electricity. It is predicted that the demand for electricity will increase in this period of time in relation to the population growth [11], increasing electricity prices and, hence, making the FOWT technology more competitive. The political commitments and agreements will also help in this regard, due to the global concerns about the need for decarbonisation.

The hydrodynamic stiffness of the platforms in FOWT systems presents a rigidity in the tower-base lower than that of the bottom-fixed or onshore wind turbines. During performance, the stability of the system can be affected by the coupling between the control of the wind turbine and the dynamics of the platform [12], exciting motions of the platform [13][14] known as platform negative damping effect [15]. This coupling produces an additional oscillatory movement of the overall FOWT system, damaging its mechanical components [16], drastically reducing its working life, and, hence, the profitability of the investment. This drawback can be overcome by mechanical means with a large and heavy floating platform. In this regard, a platform with a larger hydrostatic stiffness costs more to build [10], while a less hydrodynamically stable platform affects the FOWT's performance [17].

Therefore, the motivation for this thesis is to investigate the relation between the fundamental FOWT performance features, especially in terms of the challenges posed to the turbine control system by less hydrodynamically stable, more economical and compact platforms. This poses great challenges for the development of control algorithms able to improve the system performance, minimise the structural loads produced by wind and waves, and provides stable operation in the harsh

offshore environments. The improvement of the FOWT system performance will provide (1) alleviation of the stress suffered by the mechanical components, increasing the operational lifetime of the wind turbine, or the redesign of some components so as to make them more cost competitive, and (2) an increase in the quality and amount of energy produced per operation time. All this will make the FOWT technology more efficient and competitive, contributing to the reduction of the use of other fossil fuels and polluting energy sources, which will promote the development of a greener world.

1.3 Objectives, Scope, and Outline

The main objectives of this thesis can be summarised under three headings:

1. The reduction of the platform dynamics produced by low hydrodynamic stiffness while improving the regulation of the generator speed, so as to improve the tower and blade mechanical loads as well as the generator power quality.

2. The solution to achieve the previous objective must be cost effective and feasible, not including any additional actuator, and being implementable to different FOWT models.

3. Investigate the relation between the fundamental FOWT performance features, especially in terms of the challenges posed to the turbine control system by less hydrodynamically stable, more economical and compact platforms.

The first objective addresses the principal development problem of the FOWTs, where the platform's low hydrodynamic stiffness and the wind turbine control regulation increase the platform dynamics, leading to a deterioration of the mechanical components due to the increased loads and generator power quality due to the increased generator speed excursions. A reduction in the mechanical loads will improve the lifetime of the components and the profitability of the investment. The second objective makes the solution cost effective, not including any complex actuator, and flexible enough to be implementable in different FOWT models. The third objective aims to investigate the challenges posed to the control system by a less hydrodynamically stable, more affordable and compact platform.

Chapter 2 presents the state of the art of the FOWTs worldwide. The main floating technologies for a FOWT system are presented. The most significant FOWT projects worldwide are listed and analysed. The available simulation tools for the FOWT system are presented. The FOWT working regions, conventional baseline control, and limitations are explained. A literature review of the control techniques designed for FOWT systems previous to the development of this thesis is presented at the end of the chapter.

Chapter 3 presents the non-linear FOWT models used for the development of this thesis. The conventional linearisation process and the limitations found with the FOWT systems are explained. An alternative method that avoids the presented linearisation issue is proposed. The process carried out for designing and modelling more compact platforms is explained. The validation of the family of designed platforms is presented before continuing with the next chapter.

Chapter 4 presents the baseline controllers implemented for the FOWT models used in this thesis. The advanced control techniques design process, time- and frequency-domain performances, and load analysis are then presented. The scalability of the designed advanced control technique is demonstrated. A discussion of the results achieved with the proposed advanced control technique is given at the end of the chapter.

Chapter 5 proposes an optimisation process to improve the designed control loop and performance. The optimisation method, time- and frequency-domain performances, and load analysis are presented. A discussion of the results achieved in comparison to those of a manually designed control is provided.

In Chapter 6, the main conclusions and contributions collected during the development of this thesis and, also, some directions and recommendations for further research are suggested.

CHAPTER

2

Background for Floating Offshore Wind Technology

This chapter presents the state of the art of the FOWTs. It focuses on the current status of the FOWT technology, including the previously published scientific researches. This chapter provides a technological review to get a common point of view for the reader and the author. Furthermore, the basic wind turbine control concepts and performance for the understanding of this thesis are explained.

2.1 Floating Technologies

The floating technologies applied to the FOWTs comes from the oil & gas industry, which began using them for the design of floating stations since the 1930s, when the extraction of oil and gas was carried out in brackish coastal areas before going deeper into the open sea.

The floating technologies for FOWTs can be summarised in three main groups, globally recognised [18]: Semi-submersibles (semi-sub), Tension Leg Platform (TLP) and Spar-buoy (spar), as shown in Figure 2.1. These three main groups have been set up according to the nature of the means of mechanical stabilisation, i.e. ballast [19], hydrodynamic design [20] and taut cables [21], respectively.

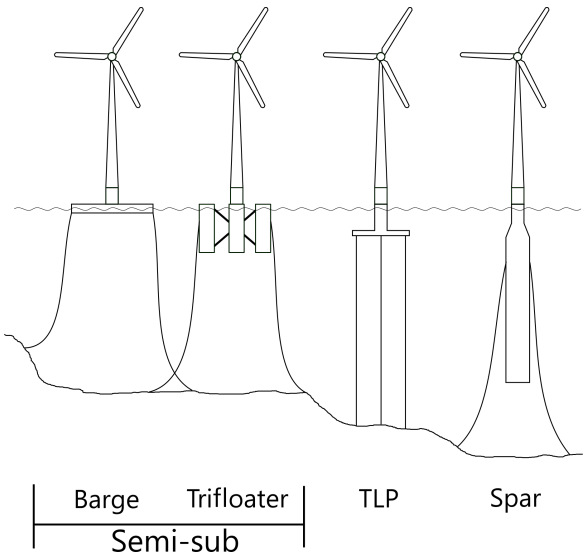

Figure 2.1: The main Floating Offshore Wind Turbine platform concepts.

The main features of these technologies are briefly explained below:

Semi-sub: With a large range of different dispositions of the floating columns and positions of the placement of the wind turbines, this technology achieves the hydrodynamic restoring via the water-plane area moment. It often requires a large structure to maintain the hydrodynamic stability, but it has a really low draft, providing the lowest minimum water depth requirement and great independence of the characteristics of the sea bed. Some loose mooring lines,

usually three or four, keeps the system on a given spot with some drift displacement freedom.

TLP: The platform is forced to be submerged through tension mooring ties fixed to the seabed. It has very high axial stiffness (low vertical elasticity) aiming to eliminate vertical motion, creating a buoyancy force to achieve the hydrodynamic restoring. Usually, a small floating structure is required, but challenges with the installation process and operational risks are frequent. Normally three to five tension lines hold the wind turbine base submerged.

Spar: The large-diameter and single vertical elongated cylinder shape (between 70 and 120 m depth approx.) submerged into the water maintains the hydrodynamic restoring, thanks to the very low centre of mass, for ballast against overturning. Thus, the centre of gravity must be lower than the centre of buoyancy to ensure the hydrodynamic stability. Some loose mooring lines, usually three, keep the system on a given spot with some drift displacement freedom. This type of platform is designed for very deep sea water areas.

According to the installation site and the involved company, the FOWT concept is stabilised by one of the mentioned floating technology, each one holding its pros and cons [22], as shown in Table 2.1. The spar platform has a very high hydrodynamic stiffness due to the large under-water structure. This hydrodynamic stability provides a good behaviour in terms of wave-induced motions. However, the huge structural dimensions and weight make its construction and installation quite difficult, which involves increased costs. The semi-sub platform has the lowest hydrodynamic stiffness due to its low draft and weight. Therefore, this floating technology present the highest sensitivity to wave-induced motions. However, it has the best advantages due to its construction and installation process, being the most economical solution since the 'concepts with the lowest steel mass have the best performance with respect to LCOE' [23]. Nevertheless, this is highly dependent on the shape of the platform and the complexity of the building. The TLP provides good hydrodynamic stiffness and low critical wave-induced motions due to its low vertical elasticity. However, difficulties have been reported in keeping system stable during transport and installation. Also, the cost of the anchoring of

this floating technology is higher than the other solutions due to the technical complexity and the seabed dependence. Furthermore, the high-frequency dynamics of the platform during the normal performance can negatively affect some components of the wind turbine.

	Semi-sub	**TLP**	**Spar**
Pitch Stability	Buoyancy	Mooring	Ballast
Natural Periods	−	+	0
Coupled Motions	−	+	0
Wave Sensitivity	−	0	+
Turbine Weight	+	0	−
Moorings	−	+	−
Anchors	+	−	+
Construction & Intallation	+	−	−
Maintenance	−	+	0

+ = relative advantage

0 = neutral

− = relative disadvantage

Table 2.1: Qualitative assessment of floating platform technologies.

Nevertheless, it is quite usual to find floating structures with a combination of these floating technologies, e.g. the TripleSpar platform [24] combines the semi-sub and spar floating technologies. This platform model takes the ballast stabilised principle from the spar platforms, but it is distributed over three columns to reduce the draft of the overall platform, as the semi-sub platforms do.

The barge-type (barge) platform is considered a submodel of the semi-sub group as it has the same means of mechanical stabilisation. However, the hydrodynamics of this platform model differs considerably from the other semi-sub platform models because of its simple and compact structural design, making it more sensitive to wave-induced motions. This platform has a purely rectangular shape with the lowest draft, where some models can include an inner pool in the middle

of the structure to increase the motion damping, such as the IDEOL's Floatgen[1] demonstrator [25]. This simple design facilitates the building process, installation, and decommissioning, which reduces the final LCOE. Apart from these improvements, the same pros and cons as those of semi-subs are hold.

There are other conceptual FOWT designs, which include more than one wind turbine in the same large semi-sub platform, i.e. multi-turbine floating platforms [26][27]. In some cases, this multi-turbine floating system can also be combined with other energy production technologies, e.g. wave [28][29] or tidal [30].

[1] https://www.ideol-offshore.com/en/floatgen-demonstrator

2.2 Projects Worldwide

A review of the past, present and near future of the worldwide FOWT and Horizontal-Axis Wind Turbine (HAWT) projects is presented here. Turbine models and projects larger than 15 kW are presented, those intended to be large scale wind turbines.

YEAR	LOCATION	NAME	TURBINE	PLATFORM	ACTUAL STATUS
2007	Apulia (Italy)	**Blue H**	80 kW	TLP	Decommissioned
2009	Karmøy (Norway)	**Hywind 1**	2.3 MW	Spar	Decommissioned
2011	Aguçadoura (Portugal)	**WindFloat**	2 MW	Semi-sub	Decommissioned
	Hordaland (Norway)	**SWAY**	15 kW	Spar	Decommissioned
2013	Maine (US)	**VolturnUS**	20 kW	Semi-sub	Decommissioned
	Nagasaki (Japan)	**Kabashima**	2 MW	Spar	Decommissioned
	Fukushima (Japan)	**Mitsui**	2 MW	Semi-sub	Operating
2016	Fukushima (Japan)	**Shimpuu**	7 MW	Semi-sub	Decommissioned
2017	Fukushima (Japan)	**Hamakaze**	5 MW	Spar	Operating
	Peterhead (Scotland)	**Hywind 2**	5 x 6 MW	Spar	Operating
2018	Saint-Nazaire (France)	**Floatgen**	2 MW	Semi-sub	Operating
	Fukuoka (Japan)	**NEDO**	3 MW	Semi-sub	Installation
	Aberdeenshire (Scotland)	**Kincardine**	2 MW	Semi-sub	Operating

Table 2.2: Floating Offshore Wind Turbine projects worldwide.

The first scaling testing Technology Readiness Level (TRL) FOWT prototype launched in the world was in 2007, named **Blue H**. It was installed 21.3 km off the coast of Apulia (Italy) and in waters with a depth of 113 m. Designed by the Dutch Blue H Technologies company, the 80 kW rated power, 2-blade and downwind configuration wind turbine was mounted on a TLP type platform. After a year of testing it was decommissioned in 2008.

The **Hywind 1** was the first large scale pre-commercial TRL FOWT. It was launched in 2009 off the south-west coast of Karmøy (Norway). Designed by Statoil (the actual Equinor), the 2.3 MW rated power and 3-blade upwind configuration wind turbine (provided by Siemens) was mounted on a spar type platform. Towed 10 km offshore into waters with a depth of 220 m, it was the first FOWT grid connected FOWT project. It was decommissioned in 2011 after a trial period.

The **WindFloat** was the first FOWT large scale pre-commercial TRL mounted in a tricolumn semi-sub type platform. It was launched in 2011 5 km off the coast of Aguçadoura (Portugal). The 3-blade upwind and 2 MW rated power wind turbine (provided by Vestas) was connected to the Portuguese electrical grid. It was decommissioned after a trial period.

In the same year, the **SWAY** scaling testing TRL FOWT was installed off the coast of Hordaland (Norway). The 3-blade downwind configuration and 15 kW rated power wind turbine was mounted on a spar floating technology platform. This FOWT included a novel system of tension rods on the upwind side reinforcing the tower and significantly reducing the steel weight of the tower as well as building cost. It was decommissioned after a trial period.

In 2013, the **VolturnUS** American first scaling testing TRL FOWT was launched off the coast of Maine (USA). The 3-blade and 20 kW rated power wind turbine was mounted on a semi-sub floating technology platform. It was decommissioned after a trial period.

In the same year, **Kabashima**, Japan's first pre-commercial FOWT, was launched off the coast of Nagasaki (Japan). The 3-blade downwind configuration and 2 MW rated power wind turbine was mounted on the first concrete spar floating platform. It was decommissioned after a trial period.

One month later, the **Mitsui** pre-commercial FOWT was installed off the coast of Fukushima (Japan). The 3-blade downwind and 2 MW rated power wind turbine was mounted on a four column compact semi-sub floating platform. At the same time, the Kizuna substation was installed in the same location on an advanced spar floating technology platform to transport the generated power to shore. Both floating systems completed the first phase of the Fukushima Floating Offshore Wind Farm Demonstration project.

In 2016, the second phase of the Fukushima project was carried out, where two FOWT pre-commercial models were installed: the **Shimpuu** with a 3-blade upwind configuration and 7 MW wind turbine mounted on a V-shape semi-sub platform, and the **Hamakaze** with a 3-blade downwind configuration and 5 MW wind turbine mounted on an advance spar platform. The installation phase was not finished until the beginning of 2017. The Shimpuu wind turbine was decommissioned in October 2018, earlier than planned, due to multiple malfunctions. There is very

little information available about the current status of the Fukushima project. The Hamakaze wind turbine is still operating.

In 2017 the **Hywind 2** first floating wind farm project (also known as Hywind Scotland Pilot Park) started operating off the Peterhead (Scotland) coast. This farm is composed of five 6 MW, 3-blade upwind configuration wind turbines, all of them mounted on spar floating platforms. The wind farm is connected to the Scottish electric grid and currently is producing more power than was expected during the design stage.

In 2018 the **Floatgen** and **NEDO** projects were being carried out in France and Japan, respectively. Both are mounted on the IDEOL's designed barge platform, which includes a damping pool in the centre of the floating concrete square structure. The first one is located in the SEM-REV testing site 22 km off the Le Croisic (France) coast in waters 30 m deep. The 3-blade upwind configuration and 2 MW wind turbine is currently being tested under real operating conditions before being decommissioned in the next year. The second one is located 15 km off the Shirashima coast (Japan) in waters of 50 m depth. The 2-blade upwind and 3 MW wind turbine is currently in the construction/installation phase.

Later, this same year, the **Kincardine** project, located 15 km off the Aberdeenshire coast in waters with a depth of 60 m, started delivering electric power to the Scottish grid in 2018. In the first phase of the project, the installation of a 3-blade upwind configuration and 2 MW wind turbine mounted on a semi-sub platform inspired by the Portuguese WindFloat project was carried out. The second phase of the project, scheduled for 2020, contemplates the installation of five 9.6 MW FOWT farm in the same location.

Apart from these pre-commercial or scale prototypes of FOWTs, several conceptual projects have been designed during these development years. The most significant ones are shown in Figure 2.2, according to the floating technology and the TRL. Sometimes, it is difficult to obtain detailed information about some projects and their development status due to the secrecy involved in these research projects.

Although all the pre-commercial or commercial level FOWT projects are mounted on semi-sub or spar type platforms, Figure 2.2 shows other scale testing level projects mounted on semi-sub platforms. This means that the involved companies

mostly bet on the semi-sub floating technology rather than the spar one. Furthermore, this figure shows that the TLP floating technology is falling behind in the TRL race. There are neither pre-commercial nor commercial level projects being developed yet with the TLP floating technology.

Figure 2.2: Worldwide Floating Offshore Wind Turbine projects according to the floating technology and Technology Readiness Level.

Several projects are currently under development. Some of them are: the previously mentioned **Kincardine** second phase project; the **DounreayTri** Hexicon multiturbine with two 5 MW wind turbines scheduled for 2020; the **NewEngland Aqua Ventus** first phase project with two 6 MW semi-sub platforms inspired by the VolturnUS prototype, to be installed in the UMaine Deepwater Offshore Wind Test Site; the **WindFloat Atlantic** project formed by three 8.4 MW wind turbines mounted on semi-sub platforms inspired by the WindFloat prototype, to be installed where the previous WindFloat pilot FOWT was decommissioned; the **Groix & Belle-Ile** floating wind pilot farm project to install four 6-MW wind turbines off France's Atlantic coast, and **Golfe du Lion**, **Eolmed**, and **Provence Grand Large** wind pilot farms projected off France's Mediterranean coast; among others.

2.3 Simulation Tools

Software for the simulation of wind turbines is based on a set of mathematical formulas to reproduce, on a computer, the performance of the system. It provides engineers with a preview of the behaviour of the designed part without running the risk of damaging a real wind turbine. For the research presented in this thesis, a simulation tool is required to test the designed control algorithms in a virtual wind turbine model. The main drawback is that the FOWTs are very complex systems, which not only include aerodynamics, structural dynamics, and servo-elastic behaviours, but also include the hydrodynamics and mooring dynamics of the floating platform. Therefore, several comprehensive testing, code-to-code comparison and validation campaigns are usually carried out. The aim of these campaigns is to check the accuracy of the simulation results with those obtained with a scaled or full FOWT prototypes. Some of these code comparison projects are known as OC3 (2005–2009) [31], OC4 (2010–2013) [32] and OC5 (2014–2018) [33]. Since the FOWT industry is quite new, more measurement data is needed to improve the code validation and simulations. Nevertheless, an actual simulations provides a very good approach to the real dynamics of the FOWT systems. The most common aero-hydro-servo-elastic simulation programs for FOWTs [34] [35], capable of performing integrated dynamic calculations, are listed in Table 2.3 below:

SOFTWARE	DEVELOPER	LICENSE
Bladed	DNV-GL	proprietary
FAST	NREL	open-source
HAWC2	DTU Risoe	proprietary
SIMPACK	SIMPACK AG	proprietary
3DFloat	UMB	proprietary
SIMO/RIFLEX	MARINTEK	proprietary
ADAMS	MSC	proprietary

Table 2.3: Floating Offshore Wind Turbine simulation programs.

Bladed, FAST, 3DFloat and HAWC2 are specific programs for the wind turbine sector, while SIMPACK, SIMO/RIFLEX and ADAMS can work for automotive, aeronautical, and robotic applications, among others. For the development of

this thesis, it was decided to use Fatigue, Aerodynamics, Structures, and Turbulence (FAST) from National Renewable Energy Laboratory (NREL) due to: (1) its great flexibility in modifying the parameters and characteristics of the FOWT model, as well as the provided simulation options and the ability to obtain linearised models; (2) the open-source nature of the software, which allows manipulating the internal formulas if necessary, the free code downloading and diffusing in the scientific community; (3) the available online FOWT models, preprocessor and postprocessor data analysis tools, and technical forum support; (4) the wide use of the software in the scientific community as evidenced by the large amount of results published in research articles found in the literature; (5) the possibility of linking the software with a Matlab/Simulink interface, enabling users to implement advanced controls with convenient block diagrams in a simple and rapid form; and (6) the positive evaluation of the FAST code by Germanischer Lloyd WindEnergy GmbH certifier [36].

FAST is a Computer-aided Aeroelastic Engineering (CAE) tool for HAWT simulation. This comprehensive aerolastic program is capable of predicting the extreme and fatigue loads of onshore, offshore bottom-fixed and FOWT systems. It joins the aerodynamic models (aero), hydrodynamic models (hydro), control and electrical system (servo) dynamics models, and structural (elastic) models to enable time-domain aero-hydro-servo-elastic simulations. It is coupled with different sub-modules for generating the wind fields (TurbSim/InfloWind) as well as computing the aerodynamics (AeroDyn) and hydrodynamics (HydroDyn), as one can see in [37] and [38].

FAST models combine the modal and multibody dynamics formulations [39]. It is formed by flexible and rigid bodies, where apart from the flexible ones, such as the tower, blades, and drivetrain, the rest are modelled as rigid. FAST has the ability to model 24 Degree Of Freedom (DOF) for a three-blade FOWT topology: three platform translational DOF (surge, sway, and heave) and three rotational (roll, pitch, and yaw)(6 DOF)(see Figure 2.3); the first and second modes of the tower fore–aft and side-to-side (4 DOF); nacelle yaw (1 DOF); variable generator and drivetrain rotational-flexibility (2 DOF); rotor- and tail-furl (2 DOF); and, the first and second flapwise modes as well as the first edgewise mode for each blade (9 DOF). Blade teetering DOF can also be enabled for a two-blade wind turbine.

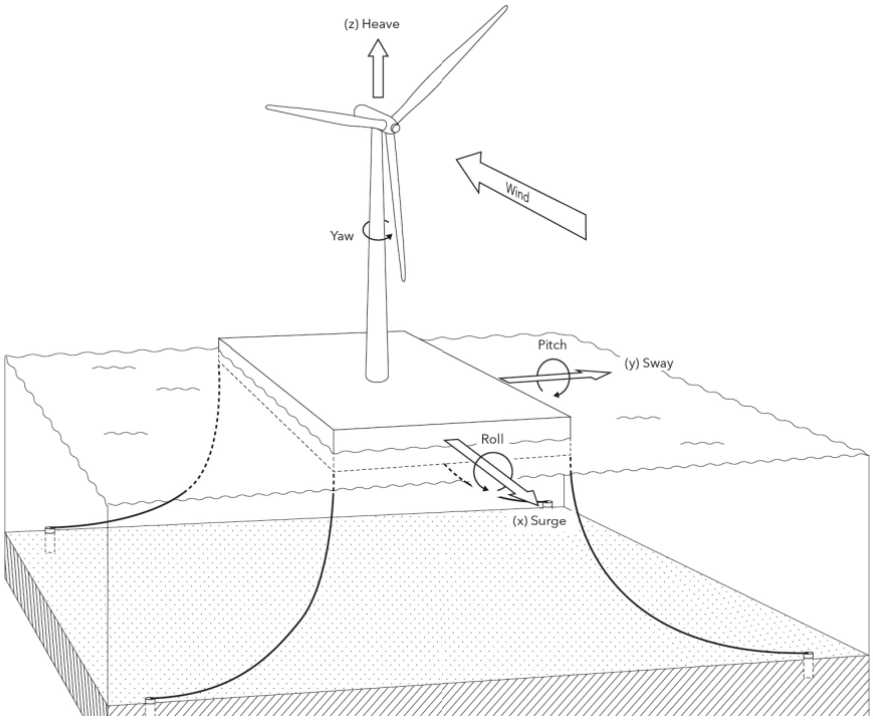

Figure 2.3: Degrees of freedom of the motion of the barge [40].

Note that the 7th version of FAST, from now on FAST7, is going to be used in this work only for the linearisation process of the FOWTs. For time-domain simulations, the 8th version of FAST, from now on FAST8, will be used. The use of FAST7 is because during the development of this thesis FAST8 does not yet have the ability to linearise FOWT models.

2.4 Control

The wind turbine control system is based on sensors, actuators and the software that links these elements [41]. The software processes the input signals from the sensors and generates output signals for the actuators. The purpose of the control is, then, to manage the right performance of the wind turbine by means of a supervisory system during all working states and conditions. The wind turbine is constantly monitored by a software program to decide which action is going to be taken next. The main objective of the control system is the trade-off between the power tracking and the fatigue load reduction while ensuring the overall integrity of the wind turbine. That is:

- Extract the maximum energy from the wind.
- Guarantee the overall integrity and correct performance of the wind turbine.
- Minimise the fatigue loads and stresses of the mechanical components.

There are four different control levels, according to the purposes of the control: the **safety control level** is the top level of the controller and is responsible of ensuring the overall integrity of the wind turbine, activating an emergency stop if necessary; the **supervisory control level** is the next level and is responsible for deciding on the operating region (see Subsection 2.4.1) of the wind turbine depending on the environmental conditions, including shut-down and power-up, enabling different components, verifying the status of the sensors, etc.; once the working region is determined, the **working control level** takes care of the generator torque and blade-pitch angle so as to extract the maximum power from the wind in each region (see Subsection 2.4.2); the last level, the **subsystem control level**, operates inside each actuator and follows the commands given by the working control level to the actuator.

This study is focused on the working control level. Nevertheless, the supervisory control level is going to be explained for the correct understanding of the working control level. The highest and lowest control levels, i.e. the safety and subsystem control levels, are not going to be analysed since that is not necessary for the achievement of the objectives of this study.

2.4.1 Operating regions

Among the huge range of different wind turbine classifications [42], the variable-speed HAWT is the most common configuration in large-scale FOWTs, including both direct-drive and gear-drive ones. In both cases, the working regions are classified according to the wind speed: stand-by, start-up, power production, shut-down and emergency stop. Figure 2.4 shows the working regions of these wind turbines.

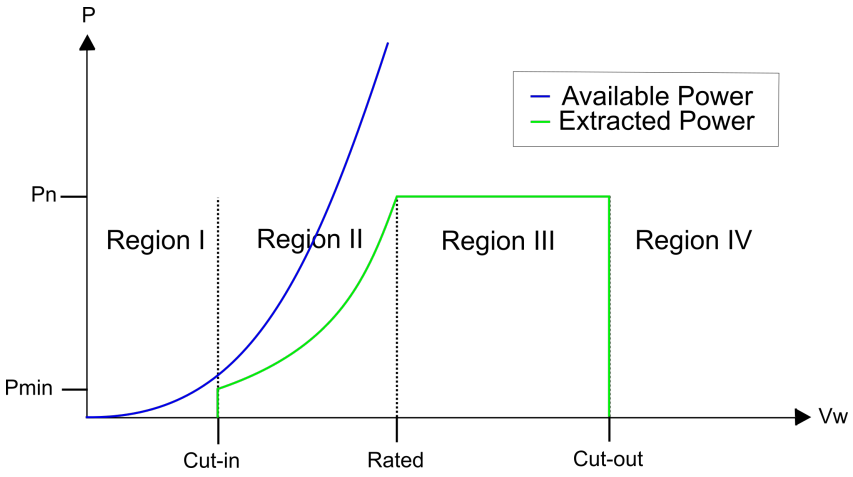

Figure 2.4: Operating regions of large scale wind turbines.

When the wind speed is below the minimum (cut-in) needed to produce electric energy, the wind turbine is kept in the **stand-by** state. In this state, the blades are in flag position and the high speed shaft is braked. The wind speed is constantly measured in case it increases sufficiently to start producing electric energy. In this case, the nacelle starts rotating its orientation to get positioned upwind before removing the high speed shaft brake.

After positioning the nacelle upwind, the **start-up** transition (Region I) sets the blade-pitch angle from the flag position (aligned to the wind direction), where the minimum thrust from the wind is produced, to an angle where the maximum thrust is produced (perpendicular to the wind direction). There is no opposing electrical torque applied to the generator, therefore it is not producing electric power but facilitating the starting of the rotation of the rotor. This state consists in achieving the

minimum rotational speed before starting to apply electrical torque to the generator and, hence, produce electric power.

Once the wind turbine is in the **power production** state, it will be working in one of the two middle regions (Regions II or III) according to the wind speed. If the wind speed spins the generator below its rated rotational velocity (below rated), then it will be working in Region II. This is also called the rotor torque region because the generator torque is being actively controlled while the blade pitch-angle is fixed at the minimum angle (usually zero degrees, perpendicular to the wind direction) to generate the highest thrust. If the wind speed is high enough that the generator speed reaches or surpasses the rated or nominal rotational velocity (above rated), then it will be working in Region III. In this region, also called the generator speed or blade-pitch control region, the blade-pitch angle is actively controlled to regulate the generator speed, trying to keep it constant at the rated value. The generator torque in this region can be kept constant at the rated value or can be inversely proportional to the generator speed to aid in the regulation of the electric power output.

If the wind exceeds the maximum tolerable speed (cut-out), then the **shut-down** process is activated in Region IV. The blades of the wind turbine increase their angle to the flag position, reducing the thrust to the minimum, to progressively decrease the generator speed. When the rotational speed is sufficiently low, then the brake is activated to block the low speed shaft and in consequence immobilise the turbine.

The **emergency stop** is only activated when a fault is detected during normal operation or in a sudden emergency action. This stop is very fast and aggressive, not being as suitable as the normal shut-down, since the wind turbine suffers considerable mechanical loads.

2.4.2 Conventional control

The conventional wind turbine control technique for Region II and Region III is based on Single-Input Single-Output (SISO) feedback loops. The Figure 2.5 represents the control scheme when the wind turbine is operating below rated wind speed (Region II). The generator torque (M_g) is set according to the generator speed (Ω_g) feedback.

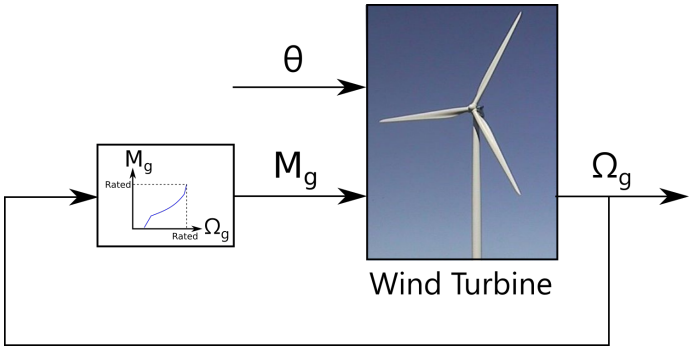

Figure 2.5: Below rated wind speed (Region II) wind turbine control loop.

In such a Region II, M_g changes proportionally to the square of Ω_g, following the optimal curve to extract the maximum power from the wind [43]. One can see that

$$\begin{aligned} M_g &= K\Omega_g^2 \\ K &= \frac{1}{2}\frac{\pi\rho R^5 C_{p_{max}}}{{\lambda_{opt}}^3 G^3} \end{aligned} \tag{2.1}$$

where ρ is the air density, R is the radius of the rotor, $C_{p_{max}}$ is the maximum power coefficient, λ_{opt} is the optimum Tip Speed Ratio (TSR), and G is the gearbox relation. The $C_{p_{max}}$ indicates the maximum power that can be extracted from the wind, which is limited by Betz's law [41] to $16/27$ (59.3%) for an ideal wind turbine. The λ is the ratio between the tangential speed of the blade tip and the current wind speed, expressed as follows:

$$\lambda = \frac{\Omega_g R}{V_w G} \tag{2.2}$$

The aerodynamic power extracted by a wind turbine can be expressed as

$$P = \frac{1}{2}\pi\rho R^2 V_w^3 Cp \tag{2.3}$$

where V_w is the wind speed.

Therefore, the ability to extract the maximum available power from the wind depends exclusively on λ, which is automatically regulated through M_g. This can be seen in Figure 2.6, where if λ is higher than the optimum value due to the wind speed is less than expected, then Ω_g drops because the aerodynamic torque is less than the opposing electric torque, M_g. If λ is less than the optimum due to the wind speed is higher than the expected, then Ω_g increases because the aerodynamic torque is more than M_g. Nevertheless, if λ is in the stall zone, the automatic regulation is lost because a higher wind speed results in a smaller aerodynamic torque. Something similar happens at very low wind speeds (below cut-in), where M_g is set to zero to let the rotor spins freely and leaves the stall zone if the wind speed is sufficient.

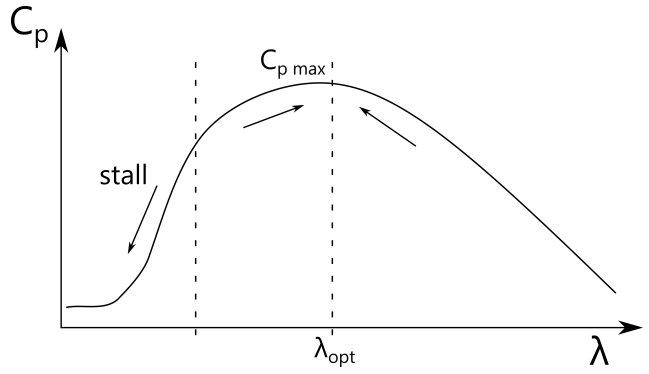

Figure 2.6: λ and C_p representation.

Depending on the wind turbine model and rated power, Region $\mathrm{I}_{1/2}$ and Region $\mathrm{II}_{1/2}$ can be implemented. Both of them consist in a linear transition between the contiguous regions based on a torque slope to aid the start-up of the wind turbine in Region $\mathrm{I}_{1/2}$, and to limit the tip speed (and, hence, the noise emissions due to the turbulence in the blade tip) in Region $\mathrm{II}_{1/2}$.

When the wind turbine is working in these regions, the blade-pitch angle (θ) is fixed to the minimum angle (close to 0°) to create the maximum thrust in the rotor and, hence, the maximum aerodynamic torque, to capture the maximum power from the wind.

When the wind turbine is operating above rated wind speed (Region III), the control scheme is as shown in Figure 2.7. In this region, C_p is below the maximum because the rated power and the nominal generator speed of the wind turbine have been reached. Thus, the objective now is to keep the generator speed constant at the rated value, by regulating the pitch angle of the blades, also known as active blade-pitch control. The value of the blade-pitch angle, θ, is set through the well known Proportional, Integral and Derivative (PID) controller according to the generator speed error (e), where the error is the difference between the reference generator speed (Ω_g^*) and the current measured generator speed. The term Proportional (P) is the proportional action, providing a control term proportional to the e, while the term Integral (I) is the integral action, providing a control term proportional to the integral over the time of such an error signal. The use of the Derivative (D) term is not recommended [44] for wind turbine control. Therefore, the Proportional and Integral (PI) controller can be expressed as

$$\theta(t) = K_p e(t) + K_i \int_0^t e(\tau) d\tau \tag{2.4}$$

$$K_i = \frac{K_p}{T_i} \tag{2.5}$$

where K_p and K_i are the proportional and integral gains, respectively, and T_i represents the integration time of the controller.

In this region, M_g can be set constant at the rated value or, if it is wanted to regulate the output power additionally to the blade-pitch PI control, then it is set inversely proportional to the generator speed, given by

$$M_g = \frac{P_n}{\Omega_g} \tag{2.6}$$

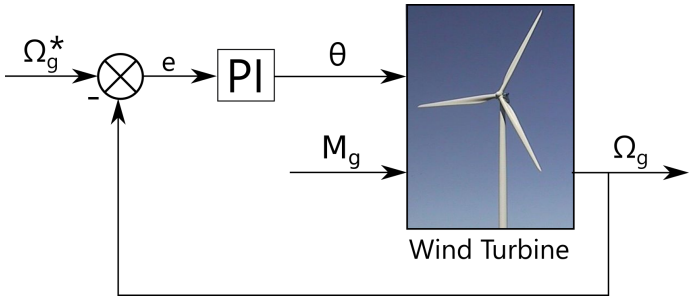

Figure 2.7: Above rated wind speed (Region III) wind turbine control loop.

where P_n is the nominal mechanical power of the wind turbine.

The proportional gain of the PI must not behave linearly, since the aerodynamic property of the wind turbine blades changes non-linearly within the above rated wind speed range. This can be seen by analysing the sensitivity of the aerodynamic power to the rotor-collective blade-pitch angle, as analysed in [15]. There, a Gain-Scheduling (GS) is proposed using the blade-pitch angle from the previous controller time step to calculate the Gain-Correction Factor (GK) at the next time step:

$$GK(\theta) = \frac{1}{1 + \frac{\theta}{\theta_K}} \tag{2.7}$$

where θ_K is the blade-pitch angle at which the pitch sensitivity has doubled from its value at the rated operating point.

Two possibilities for the implementation of the blade-pitch control are known: pitch-to-feather and pitch-to-stall [45]. The pitch-to-feather control increases the wind turbine blade-pitch angle as the wind speed increases to reduce the thrust and, hence, the generator speed. The pitch-to-stall reduces the blade-pitch angle increasing the turbulence level downwind of the blade, increasing the aerodynamic drag coefficient, resulting in a slow down of the generator speed. However, the analytical design of the pitch-to-stall algorithms is not suitable and the implementation of the GS also presents some difficulties, since the operating point of the wind turbine can not be known from the current blade-pitch angle. Thus, usually the large wind turbines, with active blade-pitch control, are pitch-to-feather controlled.

The switching between the below rated and above rated controllers is done by measuring the generator speed as well as the blade-pitch angle and saturating the PI controller, as can be seen in the flowchart in Figure 2.8. When the wind turbine is operating below rated wind speed, the generator torque is actively regulating while the error is negative due to the difference between the measured generator speed and the rated generator speed. Then the 'Integral Saturation' block (anti-windup) prevents the integrator from accumulating a negative value while the error is negative. During this region the 'Pitch Limit Saturation' block limits the proportional value to zero. When the wind turbine starts operating above rated wind speed, because the generator speed is greater than the reference one, the generator torque is fixed to rated or inversely proportional to the generator speed in Region III while the PI regulates the blade-pitch angle to keep the generator speed close to the reference. In this case, the blade-pitch angle will be working between $0°$ and $90°$, being limited by the 'Pitch Limit Saturation' block. The 'Pitch Rate Saturation' block simulates the dynamics of the maximum derivative of the blade-pitch actuator. Furthermore, the blade-pitch control will never be activated if the generator torque control is not working in Region III, and vice versa, the generator torque will not leave Region III if the blade-pitch control is actively regulating. Some

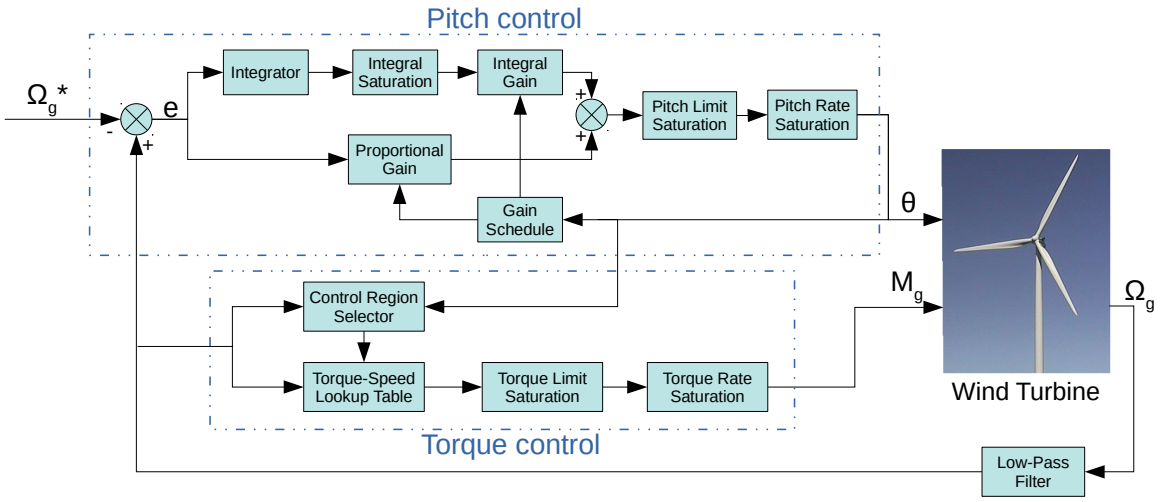

Figure 2.8: Flow chart for the conventional control of a wind turbine.

research studies are found in the literature about control switching strategies: (1) Shahsavari et al. presented an optimal Hybrid Model Predictive Control (HMPC) for switching between controllers and maximising the electrical power production in [46]; and (2) Lindeberg et al. presented a more general study of the smooth transition between controllers using the Model Predictive Control (MPC) in [47].

The blade-pitching can be done collectively or individually. Collective Pitch Control (CPC) refers to when the pitch-angle of all the blades change in unison, and Individual Pitch Control (IPC) to when the pitch-angle of each blade changes independently. The CPC is usually used as a preliminary approach to analyse the behaviour of the wind turbine, but in a more developed design stage, and with large wind turbines, the IPC is highly recommended [45]. Several benefits for the alleviation of the blade loads are attributed to the IPC strategy, such as the reduction of the effect of wind shear, tower shadow, up-flow and shaft tilt. This can be done by measuring the blade-root moments of each blade through a strain gauges.

2.4.3 Limitations of conventional control

The concern in FOWTs is that when the wind turbine is operating in Region III, and the blade-pitch PI controller is tuned as with onshore or bottom-fixed wind turbines, a coupling between the platform-pitch motion and the blade-pitch control can happen, known as platform negative damping [12][17]. This is due to the fact that the blade-pitch PI controller of the onshore and bottom-fixed wind turbines is tuned as vigorously as possible to regulate the generator speed close to the rated value and avoid speed excursions due to wind gusts, not taking into account the platform dynamics. Thus, when the wind flows, the thrust produced in the rotor of the FOWT generates a downwind motion of the system due to the platform's low hydrodynamic stiffness. During this motion, the relative wind speed observed by the wind turbine is less than the true wind speed, resulting in a slow down of the generator speed. This is measured by the control unit, which tries to keep the generator speed at the rated speed, reducing the blade-pitch angle and consequently increasing the thrust in the rotor and, hence, increases even more the downwind motion. Just the opposite happens when the FOWT is upwind. This effect may lead to large resonant platform-pitch motions, increasing blade, tower, platform and mooring line loads, as well as deteriorating the turbine performance.

In terms of control theory, this effect can be explained by analysing the root-locus of the FOWT system. The root-locus is a graphical method for representing the change of the poles and zeros of a transfer function with the variation of a system parameter. In this case, the open-loop transfer function includes the blade-pitch PI controller and the FOWT model from the blade-pitch angle to the generator speed, as shown in Figure 2.9. The analysis is focused on the platform-pitch mode

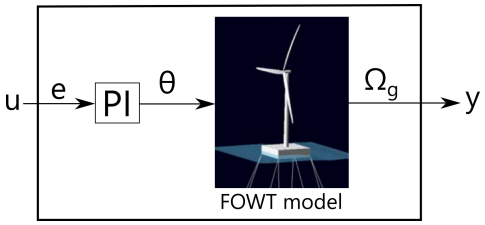

Figure 2.9: Scheme of the transfer function for the root-locus analysis.

to examine the behaviour according to the controller proportional gain variation. In this figure, a NREL 5-MW wind turbine mounted on the ITIEnergy's barge platform model, linearised at 17 m/s wind speed, is analysed. Note that the linearisation process of the FOWT is explained in Chapter 3.

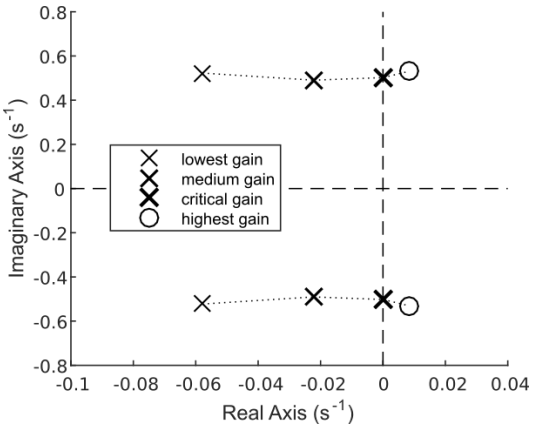

Figure 2.10: Platform-pitch mode root-locus map.

Figure 2.10 shows the locations of the poles and zeros of the platform-pitch mode of the mentioned transfer function, for a PI controller time constant of T_i= 3.5 s and for different proportional gains. The dashed line represents the path of the poles when the gain is increased from the lowest to the highest value. There, one can see how the poles go from the left half-plane of the complex plane to the right half-plane as the gain increases. Since the complex poles represent sinusoidal signals ($A \cdot e^{\gamma t} \cdot sin(\omega t + \phi)$, where A is the amplitude, γ is the propagation decay constant, t is time, ω is the angular frequency, and ϕ is the phase angle), γ must always be negative to damp that oscillation and ensure the stability of such a mode.

A pole located on the imaginary axis represents a critical stability of the platform-pitch mode, meaning that gains greater than the critical one ($K_p > 8.3 \times 10^{-4}$) will make the mode unstable (negatively damped). As shown in Figure 2.11, the blade-pitch controller-response natural frequency ($\omega_{\varphi n}$) for that critical gain is 0.083 Hz, which is very close to the ITIEnergy's barge platform-pitch natural frequency (ω_{xn} = 0.086 Hz). This supports the statement made by Larsen and Hanson [16] that for ensuring the stability of the motion of a FOWT structure, the controller-response natural frequency must be smaller than the platform-pitch natural frequency.

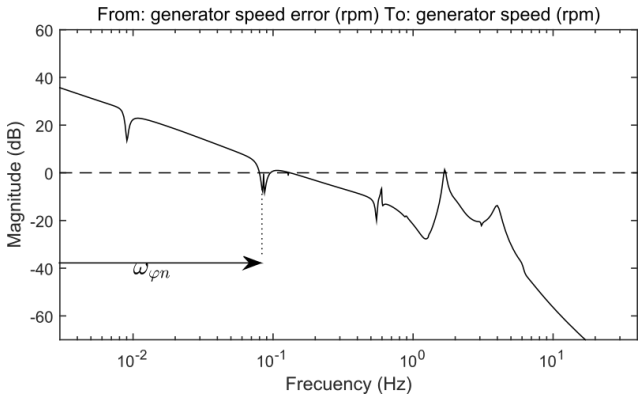

Figure 2.11: Controller-response natural frequency.

The platform negative damping effect, nevertheless, does not have the same damping over the whole wind speed range. As shown in Figure 2.9 the zero of the platform-pitch mode changes according to the thrust of the wind in the rotor of the turbine for the same controller gains. As shown in [12], the thrust has its maximum value near the rated wind speed, and decreases as the wind speed increases. This effect can be seen in the position of the zeros of the analysed transfer function in Figure 2.12, where the highest negative damping is achieved with near rated wind speed (13 m/s) and the zero position is getting closer to the left half-plane in relation to the increment of the wind speed.

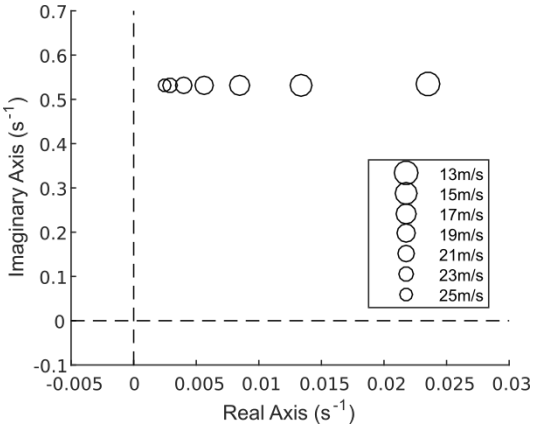

Figure 2.12: Open-loop platform-pitch zero positions according to the wind speed.

2.4.4 Review of the control literature

One of the first and most complete studies done to tackle the effect of the platform negative damping in FOWTs was carried out in [12]. Three control alternatives were proposed to mitigate the barge type platform-pitch motions: feedback the tower top acceleration, blade-pitch-to-stall regulated control, and detuned blade-pitch-to-feather gains. The best result was achieved by detuning the blade-pitch-to-feather PI controller gains. Great reductions in the platform-pitch motion and in the load on the mechanical components were achieved. However, the rapidity of the regulation of the generator speed was degraded due to the reduction in the bandwidth of the controller.

Van der Veen et al. [48] analysed the relative efficacy of the CPC feeding back the nacelle motion. Yongoon et al. [19] ensured a good FOWT performance improvement with a nacelle motion feed-back control, reducing the blade and tower loads. A similar strategy, but feeding back the nacelle velocity to the generator torque, was presented by Fischer in [49]. There, few improvements were shown in the blade and drivetrain loads with the Non-Minimum Phase Zeros (NMPZ) approach, whereas the tower fore–aft and side-to-side loads were considerably increased. Wakui et al. also feedback the nacelle velocity to the generator torque in [50]. However, the blade-pitch angle loop regulates the electric power instead of the generator speed. Few significant improvements were shown in the presented results, where the main drawback was the increase in the turbine torque activity due to the control regulation.

Wang et al. designed an active disturbance rejection control feeding back the generator speed, but regulating the electric power of the FOWT in [51]. An adaptive control law was used to weaken the impact of platform-pitching movement and compensate the perturbations by a real-time estimation with a non-linear observer. The electric power output was improved with a Proportional and Derivative (PD) control and the platform-pitch motion was reduced compared to the results obtained by using a reference baseline control. Wei et al. evaluated three different control strategies modifying the onshore baseline controllers in [52]. They concluded that all approaches have some drawbacks due to the lack of communication between

the different SISO feedbacks. They proposed an improvement of the controllers, designing a model-based Multiple-Input Multiple-Output (MIMO) control strategy.

Some other approaches can be found in the literature applying the State-Feedback (SF) control and Linear Quadratic Regulator (LQR) strategies for FOWT systems. Namik et al. [53] designed a full SF control using a LQR for a barge FOWT system. Afterwards, they implemented a periodic IPC and Disturbance-Accomodating Control (DAC) in [54] for improving the performance of the FOWT reducing the effects of the incident wind and wave disturbances. In a more recent article [55], they proposed the IPC State Space (SS) control strategy and DAC, significantly reducing the barge platform-pitch, -roll and -yaw motions, and tower loads. However, the cost of these reductions was an extensive use of the blade-pitch actuator, where the blade-pitch rate was increased by 318% compared to the conventional CPC baseline controller.

Christiansen et al. [56] designed a SF controller with a observer for the state estimation combined with a wind speed and a LQR for optimal control. The overall improvement of the spar type FOWT model performance was achieved at the cost of increasing the blade-pitch activity. The blade-pitch rate increases by 392% and the drivetrain torsion loads by 5%, in comparison to the baseline control. Their next publication [57], based in the same control technique, includes the minimum thrust and constant generator speed strategy for stabilising the floating system. Deterioration in the generator speed regulation and power production were registered as well as an increment in the platform-pitch oscillations of 20%. The last publication [58] based in the same control technique, but with an extended Kalman filter, shows the reduction of the wave disturbances on the onshore controller performance.

A more developed SF controller was developed by Zuo et al. in [59]. They proposed an additional robust adaptive control with an advanced memory-based compensation module for the IPC. The power fluctuations, fatigue loads and platform vibrations were reduced in comparison to the conventional SF controller. Bagherieh et al. presented a sliding control technique for FOWT control in [60]. In comparison to the presented baseline controller, the generator speed deviation was improved whereas the platform-pitch motions were increased considerably, increasing the blade-pitch activity. In a more recent article [61], among the different

control techniques compared, the best one for reducing the platform-pitch oscillations was the SF Linear Parameter-Varaying (LPV) GS strategy, while the best one for regulating the electric power was the LQR GS control technique. Lemmer et al. did a thorough system analysis in [62] considering the MIMO description including control inputs and disturbances in a reduced FOWT model. They demonstrated that the LQR can significantly reduce the system response and attenuate the excitation from wave disturbances.

Two authors were found using a less common control technique for FOWTs, such as fuzzy logic. Yang et al. [63] used this technique to combine the DAC and the MPC algorithms. The DAC aimed at eliminating the effect of wind disturbances and the MPC to remove the effect of wave disturbances. The proposed control with IPC shows a performance better than that of the conventional CPC. Tahani et al. also used fuzzy logic in [64] for controlling the foundation directions of the VoulturnUS FOWT model, preventing additional movements and imbalances of the wind turbine.

Some other articles treating the MPC can also be found. Schlipf et al. designed a MPC for a spar type floating FOWT in [65]. Although good improvements were shown in the shaft and blade loads, the main benefit was the reduction of the power and rotor speed standard deviation, by up to 90%. However, the cost of these improvements was a blade-pitch speed increase of about 228%. Raach et al. [66] continued in this topic, including the IPC technique to reduce the loads on the blade and minimise the yawing and pitching moments on the rotor hub. The blade loads were significantly reduced compared with those obtained by using the baseline controller. Chaaban et al. also presented the MPC but mounted on a barge platform in [67]. The results show a good overall performance improvement except in the generator power error, blade-pitch rate, and blade edgewise moment. Lemmer et al. [68] also present a study with the same control technique implemented for a double rated power capacity FOWT mounted on the TripleSpar platform. The results show that the MPC damps the tower-top and platform-pitch motion better than the presented baseline PI controller and reduces significantly the overshoot of the rotor speed.

The robust H-infinity (H_∞) control method is widely extended in FOWT systems too. Bakka et al. used the H_∞ feedback control technique with pole placement

constraints in [69] and [70], with a LPV FOWT model. The generator speed and torque oscillations as well as the platform fore-aft displacement were reduced, but the blade-pitch activity was considerably increased. They used a similar technique in [71], but combining the H_2 and H_∞ control techniques, resulting in a good rotor speed regulation and a tower-top displacement mitigation but increasing considerably the blade-pitch activity as well. Betti et al. also used the H_∞ control technique for spar and TLP mounted FOWTs in [72] and [21], respectively. Navalkar et al. presented a combination of feedback and feedforward control using the H_∞ criterion in [73]. They implemented the Light Detection and Ranging (LIDAR) technology for the feedforward control enabling the wind turbine for the measurement of the incoming wind. Hara et al. presented experimental results from a scaled model FOWT using the H_∞ loop-shaping control in [74]. In comparison to the presented baseline PI control, the rotor speed regulation and platform-pitch oscillation were slightly improved whereas the blade-pith activity was considerably increased.

Lackner presented the Variable Power Pitch Control (VPPC) technique in [75] and [76]. This control technique consists in changing the generator speed set point to a larger value when the platform is pitching upwind, and vice versa. The platform motion is improved. However, the blade-pitch rate is considerably increased, by around 40%.

Other interesting articles can be found in the FOWT literature, not directly related with the negative platform damping control issue, but which some readers may find of interest. Han et al. studied a method to compute the movable range as well as the position control of FOWT systems in [77]. There are a couple of articles about a novel control technique for Region II. First, Bagherieh et al. used the blade-pitch control for this region in [20]. Second, Wang et al. used a variable torque control using an advanced Radial Basis Function (RBF) neural network in [78].

2.5 Summary

Three main types of floating support structures have been presented for FOWT systems in Section 2.1. Taking into account the TRL analysis of the worldwide projects of Section 2.2, the following summary can be made: (1) The semi-sub is the most widely used floating support structure, being a promising solution due to its advantages regarding to the fabrication, mounting and towing. Unfortunately, it has the lowest hydrodynamic stiffness, resulting in a high sensitivity to the control performance and wave induced motions. (2) The spar floating technology is slightly less used, probably due to the high investment required for building the platform, and the high complexity of the process of mounting the wind turbine. However, it has the highest hydrodynamic stiffness and lowest sensitivity to the control performance and wave induced motions, which imposes fewer requirements on the control. (3) The TLP technology is the least used floating solution, mainly due to the difficulties presented in its transportation and installation as well as the elevated anchoring risk and cost. Therefore, the semi-sub floating platform has been chosen as the most suitable floating technology for the development of this research due to the challenges posed to the control requirements needed to counteract the low hydrodynamics stiffness and, at the same time, reduce the high sensitivity to the control performance and wave induced motions. This would alleviate the drawbacks of the semi-subs, contributing to the advantages presented by this floating technology and making it more competitive.

The simulation tool FAST has been found very appropriate for the development of this thesis due to the advantages presented in Section 2.3, briefly: (1) its high flexibility; (2) its open-source code; (3) the available online support; (4) its wide use in the scientific community; (5) the possibility of linking it with Matlab/Simulink; and (6) its positive code certification. FAST8 has been used for the development of the time-domain simulations whereas FAST7 has been used only for the FOWT linearisation process.

In the FOWT control literature review, several key notes have been collected: (1) blade-pitch control detuning avoids the negative platform damping effect due to the reduction in the controller bandwidth below the critical platform-pitch natural frequency. However, this controller bandwidth reduction degrades the regulation of

the generator speed, directly affecting the produced electric power quality; (2) several studies have attempted to optimise the PI controller through different optimal control approaches or methods, such as LQR or H_∞. However, in the majority of the studies, there is a considerable increase in the blade-pitch activity, and, in some cases, a little improvement and/or even a deterioration of the mechanical loads suffered by the wind turbine blades or tower were reported. Good results have been achieved with the MPC technique in the reduction of the blade loads, but an increase in the blade-pitch activity has been shown; (3) the selection of the controller type can be highly dependent on the floating technology, e.g. the H_∞ control strategy is only implemented in the spar and TLP platforms, which have a high hydrodynamic stiffness and low sensitivity to the controller induced platform motions; and (4) the results of different considerations have been collected with the nacelle feedback control method, improving the blade and tower loads in some cases, and showing a performance deterioration in others. Therefore, after analysing the different control methods and performances, it can be summarised that complex mathematical control algorithms show a high increase in the blade-pitch activity, an uncertain efficacy in the reduction of the mechanical loads, and the controllers robustness is not guaranteed [79]. Thus, in this thesis, it has been decided to resort to the basis of the control design that analyses the Bode diagrams of the system and manually shapes the transfer functions to ensure the desired system response. In this way, the obtained performance results can be analysed and evaluated in terms of the efficacy of the proposed control method, determining whether it is acceptable or not while comparing them to the performance results of the more mathematically complex FOWT controllers.

CHAPTER

6

Conclusions and Recommendations

This chapter summarises the main conclusions and contributions collected during the development of this thesis and, also, some recommendations for further research are suggested.

6.1 Conclusions

The offshore wind energy presents the potential to become the real alternative of fossil fuels in the near future and, since the LCOE of the floating wind technology will be reduced to competitive levels, the wind energy harvesting in deepwater areas will become feasible. The amount of worldwide lunched FOWT prototypes, the first floating pilot park and the many currently developing projects show the interest in the floating wind technology, as presented in Chapter 2. Nevertheless, greater engineering efforts have to be carried out to achieve the final design in relation to the FOWT hydrodynamic stability, manufacturing cost reduction and performance quality improvement.

This thesis contributes to the performance improvement of the FOWTs reducing the tower and blade DELs via a feedback control technique, which is a technically feasible and economically affordable solution. In Chapter 4 an advanced control technique has been presented. Remarkable results have been achieved with the DTU 10-MW TripleSpar FOWT model in the overall above rated wind speed and sea state conditions, where both the loads of the platform-base and blade-roots have been successfully reduced below the reference. However, a high influence of the platform hydrodynamic stability on the APS controller performance has been registered as shown by the NREL 5-MW ITI Energy's and more compact barge platform FOWT models. The NREL 5-MW ITI Energy's barge FOWT model shows an effective APS control performance in the overall wind speed range under still and smooth sea state conditions. However, in rough sea state conditions, the wave induced platform motions highly influence the APS controller performance increasing the blade loads. Therefore, an additional feedback control loop has been designed to counteract the negative effect of the waves, i.e. the WR control loop. The implementation of the WR controller improves the blades loads below the reference Detuned PI results, slightly increasing the loads in the tower. Furthermore, the challenge of the APS controller to perform in a less hydrodynamically stable and more compact platform has been investigated. From a certain beam-draught ratio onwards, a great control potential for the FOWT performance improvement has seen. However, an additional control loop will be required to counteract the increment of the platform-roll dynamics.

Moreover, a non-linear model based optimisation process to further improve the manually tuned APS and WR control loops designed for the NREL 5-MW ITI Energy's barge FOWT model has been presented in Chapter 5. This innovative control optimisation proposes the automatisation of the feedback control loop tuning process based on DEL results. The implementation of this optimisation method achieves significant improvements of the DELs in regards to the manually tuned controller results while maintaining the time-domain performance. All the DEL results have been reduced below those of the reference Detuned PI controller for wind speeds from 17 m/s to above, reaching a maximum reduction of nearly 20% in tower-base-pitch and 12% in blade-root-flapwise. Such a fact points out the potential effectiveness of the designed advanced control technique for the improvement of the FOWT performance. Then, it validates the contribution of the novel proposed optimisation methodology for tuning feedback control loops in FOWT systems.

The issue of the FAST7 software in regard to the linearisation process with low hydrodynamic stability platforms affected by the negative damping has been presented in Chapter 3. Two alternatives to the conventional linearisation methods have been proposed: (1) trimming the generator torque; and (2), the chirp signal methodology. The first provides acceptable linear models while the second one delivers the highest fidelity results respect to the identification of the system modes, contributing with a novel method for linearising FOWT systems. Additionally, this thesis has explored the potential of an open-source modelling code NEMOH for getting the hydrodynamic matrices of the designed more compact barge family, achieving accurate results in comparison to the more conventional codes validating the approach from the method development point of view.

In summary of the accomplishments, the objectives of the thesis have been satisfied (1) improving the overall FOWT performance while reducing the tower and blade mechanical loads (2) by means of control techniques, which are scalable to different FOWT models, and (3) analysing the designed control performance in a more compact barge family. It is believed that the study presented in this thesis would contribute to the common goal of reaching the final FOWT concept solution and, supplying electric power from the deepwater areas to much of the world.

6.2 Recommendations

The linearisation process for FOWT systems will be included soon in OpenFAST code, which will include the waves as a disturbance input. Then, this would be helpful for analysing the APS control loop performance under the wave disturbance and for further reducing the system DEL results by means of the control tuning.

An extra study would include the addition of the barge platform dimensions in the presented optimisation methodology. This could help in the achievement of an optimised barge model according to the advanced controller and, in the further improvement of the FOWT performance.

The implementation of the IPC is strongly recommended due to the advantages cited in Subsection 2.4.2. Concretely, such an implementation will alleviate the blade loads, providing a retuning of the APS and WR controllers and, hence, the chance to further improve the tower loads.

An additional platform-roll control loop is required for the NREL 5-MW model mounted on a more compact beam-draught ratio 8 barge, as shown in Subsection 4.2.2.2. In this way, it is believed that the APS can provide a similar performance to that of the ITI Energy's barge platform, taking into account the physical limitations, such as, the higher static platform-pitch inclination of a more compact barge.

It would be beneficial to expand the considered set of simulation cases for a more realistic wind and wave conditions, including wind and wave misalignment, according to one specific location including the on site collected environmental data. This will allow a thorough load study of the mechanical components determining where the controller efforts should be focused on. In this case, if the advanced controller results would be positive, it should be validated in a wave-tank test, first, and in a sub- and full-scale prototype installed offshore, next.

The optimisation of the APS controller with the DTU 10-MW TripleSpar FOWT model would be recommendable to quantify the controller potential for the performance improvement.

For future works, the use of the reduced order and high fidelity FOWT models for the optimisation method presented in this thesis would be recommendable. This would decrease the computational time and give the chance to include additional

partial terms in the cost functions. Also, the optimisation process under the collected environmental real data of the specific location where the FOWT is going to be installed would help the achievement of the best control parameter values for that specific location.

Although this thesis is focused on the development of an advanced control technique for above rated wind speed region, control switching issues have been registered between the below and above rated controllers when the wind turbine is operating near rated. Therefore, a general recommendation is done for the development of an advanced switching mechanism for the transitions of these two controllers, which is out of the scope of this thesis, that will improve the performance of the wind turbine when operating near rated.

Bibliography

[1] International Energy Agency (IEA), "Renewables information: Overview 2017," tech. rep., 2017. 2

[2] Wind Europe, "Offshore Wind in Europe - Key trends and statistics 2017," tech. rep., 2018. 2

[3] P. A. Lynn, *Onshore and Offshore Wind Energy*. Wiley, 2011. 2

[4] M. Bilgili, A. Yasar, and E. Simsek, "Offshore wind power development in Europe and its comparison with onshore counterpart," *Renewable and Sustainable Energy Reviews*, vol. 15, no. 2, pp. 905–915, 2011. 3

[5] W. Musial, S. Butterfield, and B. Ram, "Energy From Offshore Wind," *Offshore Technology Conference*, 2006. 3

[6] W. De Vries, "Final report WP4.2: Support Structure Concepts for Deep Water Sites," tech. rep., 2011. 3

[7] S. Butterfield, W. Musial, J. Jonkman, and P. Sclavounos, "Engineering Challenges for Floating Offshore Wind Turbines," *Offshore Wind Conference*, p. 13, 2005. 3

[8] L. Kilar, "Offshore Wind Energy Conversion System: Preview Of A Feasibility Study," in *Third Biennial Conf. & Workshop On Wind Energy Conversion Systems*, (Washington D.C., U.S.A.), 1977. 3

[9] J. Dixon and R. Swift, *Offshore Wind Turbines: Platform Kinematics*. BHRA Fluid Engng, 1981. 3

[10] M. Kausche, F. Adam, F. Dahlhaus, and J. Großmann, "Floating offshore wind - Economic and ecological challenges of a TLP solution," *Renewable Energy*, vol. 126, pp. 270–280, 2018. 5

[11] G. Koreneff, M. Ruska, J. Kiviluoma, J. Shemeikka, B. Lemström, R. Alanen, and T. Koljonen, *Future development trends in electricity demand*. No. 2470, VTT Tiedotteita - Valtion Teknillinen Tutkimuskeskus, 2009. 5

[12] J. Jonkman, "Influence of Control on the Pitch Damping of a Floating Wind Turbine," in *46th AIAA Aerospace Sciences Meeting and Exhibit*, p. 1306, ASME, 2008. 5, 30, 32, 33

[13] R. Ramos, "Optimal Vibration Control of Floating Wind Turbines in the Presence of Nonlinearities," in *32nd International Conference on Ocean, Offshore and Arctic Engineering*, ASME, 2013. 5

[14] A. Jose, J. Falzarano, and H. Wang, "A Study Of Negative Damping In Floating Wind Turbines Using Coupled Program FAST-SIMDYN," *1st International Offshore Wind Technical Conference (IOWTC), American Society of Mechanical Engineers (ASME)*, 2018. 5

[15] J. Jonkman, "Dynamics modeling and loads analysis of an offshore floating wind turbine," tech. rep., 2007. xxv, 5, 27, 41, 42, 58, 62, 63, 73, 79, 115, 119, 140

[16] T. Larsen and T. D. Hanson, "A method to avoid negative damped low frequent tower vibrations for a floating, pitch controlled wind turbine," in *Journal of Physics: Conference Series*, vol. 75, IOP Publishing, 2007. 5, 31

[17] E. Wayman and P. Sclavounos, "Coupled Dynamic Modeling of Floating Wind Turbine Systems," in *Offshore Technology Conference*, 2006. 5, 30, 105

[18] C. Ng and L. Ran, *Offshore Wind Farms: Technologies, Design and Operation*. Woodhead Publishing Series in Energy: Number 92, 2016. 10

[19] O. Yongoon, K. Kwansu, K. Hyungyu, and P. Insu, "Control Algorithm of a Floating Wind Turbine for Reduction of Tower Loads and Power Fluctuation," *International Journal of Precision Engineering and Manufacturing*, 2015. 10, 33

[20] O. Bagherieh and R. Nagamune, "Utilization of Blade Pitch Control in Low Wind Speed for Floating Offshore Wind Turbines," in *American Control Conference (ACC)*, 2014. 10, 36

[21] G. Betti, M. Farina, G. A. Guagliardi, A. Marzorati, and R. Scattolini, "Development of a Control-Oriented Model of Floating Wind Turbines," *IEEE Transactions on Control Systems Technology*, vol. 22, no. 1, 2014. 10, 36

[22] J. Jonkman and D. Matha, "A Quantitative Comparison of the Responses of Three Floating Platforms," in *European Offshore Wind Conference and Exhibition*, 2010. 11

[23] A. Myhr, C. Bjerkseter, A. Ågotnes, and T. A. Nygaard, "Levelised cost of energy for offshore floating wind turbines in a lifecycle perspective," *Renewable Energy*, vol. 66, pp. 714–728, 2014. 11

[24] J. Azcona, F. Vittori, U. Schmidt Paulsen, F. Savenije, G. Kapogiannis, X. Karvelas, D. Manolas, S. Voutsinas, F. Amann, R. Faerron-Guzmán, and F. Lemmer, "INNWIND.EU D4.3.7: Design solutions for 10MW floating offshore wind turbines," tech. rep., CENER, 2017. 12, 54

[25] A. Alexandre, Y. Percher, T. Choisnet, R. Buils Urbano, and R. Harries, "Coupled Analysis and Numerical Model Verification for the 2MW Floatgen Demonstrator Project With IDEOL Platform," in *ASME 2018 1st International Offshore Wind Technical Conference*, ASME, nov 2018. 13

[26] Y. H. Bae and M.-H. Kim, "The Dynamic Coupling Effects of a MUFOWT (Multiple Unit Floating Offshore Wind Turbine) with Partially Broken Blade," *Wind Energy*, vol. 2, no. 2, pp. 89–97, 2015. 13

[27] C. Röckmann, S. Lagerveld, and J. Stavenuiter, *Aquaculture Perspective of Multi-Use Sites in the Open Ocean*. Springer International Publishing, 2017. 13

[28] A. Yde, M. M. Pedersen, S. B. Bellew, and E. al., "Experimental and Theoretical Analysis of a Combined Floating Wave and Wind Energy Conversion Platform," tech. rep., DTU Wind Energy, 2014. 13

[29] C. Pérez-Collazo, D. Greaves, and G. Iglesias, "A review of combined wave and offshore wind energy," *Renewable and Sustainable Energy Reviews*, vol. 42, pp. 141–153, 2015. 13

[30] D. Lande-Sudall, T. Stallard, and P. Stansby, "Co-located offshore wind and tidal stream turbines: Assessment of energy yield and loading," *Renewable Energy*, vol. 118, pp. 627–643, 2018. 13

[31] J. Jonkman, "Definition of the Floating System for Phase IV of OC3," tech. rep., 2010. 18

[32] W. Popko, F. Vorpahl, A. Zuga, and E. Al., "Offshore Code Comparison Collaboration Continuation (OC4), Phase I—Results of Coupled Simulations of an Offshore Wind Turbine with Jacket Support Structure," in *22nd International Society of Offshore and Polar Engineers Conference*, 2012. 18

[33] A. N. Robertson, F. Wendt, J. M. Jonkman, and E. Al., "OC5 Project Phase II: Validation of Global Loads of the DeepCwind Floating Semisubmersible Wind Turbine," in *14th Deep Sea Offshore Wind R&D Conference*, EERA, 2017. 18

[34] A. Cordle and J. Jonkman, "State of the Art in Floating Wind Turbine Design Tools," in *International Offshore and Polar Engineering*, 2011. 18

[35] J. Jonkman and A. Cordle, "State of the art in design tools for floating offshore wind turbines," Tech. Rep. March, Deliverable Report Under (SES6), UoWind project, Bristos, UK, 2010. 18

[36] A. Manjock, "Design Codes FAST and ADAMS® for Load Calculations of Onshore Wind Turbines," tech. rep., 2005. 19

[37] D. Matha and M. Kühn, "Model Development and Loads Analysis of a Wind Turbine on a Floating Offshore Tension Leg Platform," *European Offshore Wind Conference*, 2009. 19

[38] B. J. Jonkman and J. M. Jonkman, "FAST v8.16.00a-bjj," tech. rep., NREL, 2016. 19

[39] J. M. Jonkman and J. M. L. Buhl, "FAST User ' s Guide," tech. rep., 2005. 19, 40, 44, 45, 55, 91

[40] "DNVGL-ST-0119 Design of Floating Wind Turbine Structures," tech. rep., DNV-GL, 2018. xxv, 20, 99, 122, 123

[41] T. Burton, D. Sharpe, N. Jenkins, and E. Bossanyi, *Wind Energy Handbook*. Chichester, UK: John Wiley & Sons, Ltd, 2001. 21, 24

[42] W. Tong, *Wind Power Generation and Wind Turbine Design*. WIT Press, 2010. 22

[43] E. Bossanyi, "The Design of closed loop controllers for wind turbines," *Wind Energy*, vol. 3, 2000. 24

[44] M. H. Hansen, A. Hansen, T. J. Larsen, S. Oye, P. Sorensen, and P. Fuglsang, "Control design for a pitch-regulated, variable speed wind turbine," tech. rep., 2005. 26, 73

[45] E. A. Bossanyi, "Wind Turbine Control for Load Reduction," *Wind Energy*, vol. 6, 2003. 27, 29

[46] B. Shahsavari, O. Bagherieh, N. Mehr, R. Horowitz, and C. Tomlin, "Optimal Mode-Switching and Control Synthesis for Floating Offshore Wind Turbines," in *American Control Conference (ACC)*, 2016. 29

[47] E. Lindeberg, H. G. Svendsen, and K. Uhlen, "Smooth transition between controllers for floating wind turbines," *Energy Procedia*, vol. 24, 2012. 29

[48] G. van der Veen, I. Couchman, and R. Bowyer, "Control of floating wind turbines," *American Control Conference (ACC)*, pp. 3148–3153, 2012. 33

[49] B. Fischer, "Reducing rotor speed variations of floating wind turbines by compensation of non-minimum phase zeros," *Renewable Power Generation, IET*, vol. 7, pp. 413–419, 2013. 33

[50] T. Wakui, M. Yoshimura, and R. Yokoyama, "Multiple-Feedback Control of Power Output and Platform Pitching Motion for a Floating Offshore Wind Turbine-Generator System," *Energy*, 2017. 33

[51] L. Wang, H. Zhang, M. Cai, and Z. Luo, "Active Disturbance Rejection Power Control for a Floating Wind Turbine," in *Chinese Control And Decision Conference (CCDC)*, 2017. 33

[52] W. Yu, F. Lemmer, D. Schlipf, P. W. Cheng, B. Visser, H. Links, N. Gupta, S. Dankemann, B. Counago, and J. Serna, "Evaluation of control methods for floating offshore wind turbines," in *DeepWind, 15th Deep Sea Offshore Wind R&D Conference*, EERA, 2018. 33, 72, 125

[53] H. Namik, K. A. Stol, and J. Jonkman, "State-space control of tower motion for deepwater floating offshore wind turbines," *AIAA Aerospace Sciences Meeting and Exhibit*, 2008. 34

[54] H. Namik and K. A. Stol, "Disturbance Accommodating Control of Floating Offshore Wind Turbines," *AIAA Aerospace Sciences Meeting including The New Horizons Forum and Aerospace Exposition*, 2009. 34

[55] H. Namik and K. A. Stol, "Performance analysis of individual blade pitch control of offshore wind turbines on two floating platforms," *Mechatronics*, 2011. 34

[56] S. Christiansen, T. Knudsen, and T. Bak, "Optimal Control of a Ballast-Stabilized Floating Wind Turbine," in *IEEE International Symposium on Computer-Aided Control System Design (CACSD)*, IEEE, sep 2011. 34

[57] S. Christiansen, T. Bak, and T. Knudsen, "Minimun Thrust Load Control for Floating Wind Turbine," *IEEE International Conference on Control Applications (CCA)*, 2012. 34

[58] S. Christiansen, T. Knudsen, and T. Bak, "Extended Onshore Control of a Floating Wind Turbine with Wave Disturbance Reduction," in *The Science of Making Torque from Wind*, 2014. 34

[59] S. Zuo, Y. D. Song, L. Wang, and Q.-w. W. Song, "Computationally Inexpensive Approach for Pitch Control of Offshore Wind Turbine on Barge Floating Platform," *The Scientific World Journal*, 2013. 34

[60] O. Bagherieh and K. Hedrick, "Nonlinear Control of Floating Offshore Wind Turbines Using Input / Output Feedback Linearization and Sliding Control," in *ASME Dynamic Systems and Control Conference*, 2014. 34

[61] O. Bagherieh and R. Nagamune, "Gain-scheduling control of a floating offshore wind turbine above rated wind speed," *Control Theory and Technology*, 2015. 34, 72

[62] F. Lemmer, D. Schlipf, and P. W. Cheng, "Control design methods for floating wind turbines for optimal disturbance rejection," in *The Science of Making Torque from Wind*, vol. 753, IOP Publishing, 2016. 35

[63] F. Yang, Q.-w. Song, L. Wang, S. Zuo, and S.-s. Li, "Wind and Wave Disturbances Compensation to Floating Offshore Wind Turbine Using Improved Individual Pitch Control Based on Fuzzy Control Strategy," *Abstract and Applied Analysis*, 2014. 35

[64] M. Tahani, E. Ziaee, A. Hajinezhad, P. Servati, M. Mirhosseini, and A. Sedaghat, "Vibrational simulation of offshore floating wind turbine and its directional movement control by fuzzy logic," in *International Conference on Sustainable Mobility Applications, Renewables and Technology (SMART)*, IEEE, nov 2015. 35

[65] D. Schlipf, F. Sandner, S. Raach, D. Matha, and P. W. Cheng, "Nonlinear model predictive control of floating wind turbines," *International Offshore and Polar Engineering*, vol. 9, pp. 440–446, 2013. 35

[66] S. Raach, D. Schlipf, F. Sandner, D. Matha, and P. W. Cheng, "Nonlinear Model Predictive Control of Floating Wind Turbines with Individual Pitch Control," in *American Control Conference (ACC)*, (Portland, Oregon (USA)), 2014. 35

[67] R. Chaaban and C.-P. Fritzen, "Reducing Blade Fatigue and Damping Platform Motions of Floating Wind Turbines Using Model Predictive Control," in *International Conference on Structural Dynamics EURODYN*, 2014. 35

[68] F. Lemmer, S. Raach, D. Schlipf, and P. W. Cheng, "Prospects of Linear Model Predictive Control on a 10 MW Floating Wind Turbine," in *International Conference on Ocean, Offshore and Arctic Engineering*, 2015. 35

[69] T. Bakka and H. R. Karimi, "Robust H∞ Dynamic Output Feedback Control Synthesis with Pole Placement Constraints for Offshore Wind Turbine Systmes," *Mathematical Problems in Engineering*, 2012. 36

[70] T. Bakka and H. R. Karimi, "Robust Output Feedback H∞ Control Synthesis with Pole Placement for Offshore Wind Turbine System: An LMI Approach," in *International Conference on Control Applications (CCA)*, 2012. 36

[71] T. Bakka and H. R. Karimi, "Mixed H2/H∞ Control Design for Wind Turbine System with Pole Placement Constraints," in *Chinese Control Conference*, 2012. 36

[72] G. Betti, M. Farina, A. Marzorati, R. Scattolini, and G. A. Guagliardi, "Modeling and control of a floating wind turbine with spar buoy platform," in *International Energy Conference and Exhibition (ENERGYCON)*, 2012. 36

[73] S. T. Navalkar, J. W. Van Wingerden, P. A. Fleming, and G. A. M. Van Kuik, "Integrating robust Lidar-Based Feedforward with Feedback Control to Enhance Speed Regulation of Floating Wind Turbines," in *American Control Conference*, IEEE, 2015. 36

[74] N. Hara, Y. Nihei, K. Iijima, and K. Konishi, "Blade Pitch Control for Floating Wind Turbines: Design and Experiments Using a Scale Model," in *Control Technology and Applications (CCTA)*, IEEE, 2017. 36

[75] M. A. Lackner, "Controlling Platform Motions and Reducing Blade Loads for Floating Wind Turbines," *Wind Engineering*, vol. 33, no. 6, pp. 541–553, 2009. 36, 79

[76] M. A. Lackner, "An investigation of variable power collective pitch control for load mitigation of floating offshore wind turbines," *Wind Energy*, vol. 16, no. 3, pp. 435–444, 2013. 36, 80

[77] C. Han, J. R. Homer, and R. Nagamune, "Movable Range and Position Control of an Offshore Wind Turbine with a Semi-submersible Floating Platform," in *American Control Conference (ACC)*, 2017. 36

[78] L. Wang, S. Zuo, Y. D. Song, and Z. Zhou, "Variable Torque Control of Offshore Wind Turbine on Spar Floating Platform Using Advanced RBF Neural Network," *Abstract and Applied Analysis*, 2014. 36

[79] S. Skogestad and I. Postlethwaite, *Multivariable Feedback Control: Analysis and Design*. John Wiley & Sons, 2nd ed., 2001. 38

[80] J. Olondriz, I. Elorza, I. Trojaola, A. Pujana, and J. Landaluze, "On the effects of basic platform design characteristics on floating offshore wind turbine control and their mitigation," in *The Science of Making Torque from Wind*, IOP Publishing, 2016. xxvi, 39, 59, 60, 63, 65, 71

[81] J. Olondriz, J. Jugo, I. Elorza, S. Alonso-Quesada, and A. Pujana-Arrese, "Alternative linearisation methodology for aero-elastic Floating Offshore Wind Turbine non-linear models," in *The Science of Making Torque from Wind*, IOP Publishing, 2018. xxv, xxvi, xxxi, 39, 50, 52, 53

[82] J. Olondriz, W. Yu, J. Jugo, F. Lemmer, I. Elorza, S. Alonso-Quesada, and A. Pujana-Arrese, "Using multiple fidelity numerical models for floating offshore wind turbine advanced control design," *Energies*, vol. 11, no. 9, pp. 2484–2497, 2018. 39, 71, 112

[83] K. J. Amstrong and R. M. Murray, *Feedback Systems: An Introduction for Scientists and Engineering*. Princeton university press, 2010. 40

[84] K. Ogata, *Ingeniería de Control Moderna*. Pearson Education, 5th ed., 2010. 40

[85] P. H. Jensen, T. Chaviaropolos, and A. Natarajan, "LCOE reduction for the next generation offshore wind turbines," tech. rep., 2017. 41

[86] F. Lemmer, K. Müller, Y. Wei, D. Schlipf, and P. W. Cheng, "Optimization of Floating Offshore Wind Turbine Platforms With a Self-Tuning Controller," in *Internationl Conference on Ocean, Offshore and Arctic (OMAE)*, ASME, 2017. xxv, 42, 140

[87] A. Raizada, V. Krishnakumar, and P. Singru, "System Identification : A Study Of Various Methods For Continuous Systems," in *International and National Conference on Machines and Mechanisms (iNaCoMM)*, 2015. 49

[88] R. Pintelon and J. Schoukens, *System Identification: A Frequency Domain Approach*. John Wiley & Sons, Inc., 2004. 49

[89] S. W. Smith, *The Scientist and Engineer's Guide to Digital Signal Processing*. California Technical Publishing, 1997. 51

[90] F. Lemmer, "Multibody Modeling for Concept-Level Floating Offshore Wind Turbine Design," *Multibody System Dynamics*, 2018. 54

[91] F. Lemmer (né Sandner), S. Raach, D. Schlipf, and P. W. Cheng, "Parametric Wave Excitation Model for Floating Wind Turbines," *Energy Procedia*, vol. 94, pp. 290–305, sep 2016. 54

[92] F. Sandner, D. Schlipf, D. Matha, and P. W. Cheng, "Integrated Optimization of Floating Wind Turbine Systems," in *International Conference on Ocean, Offshore and Arctic Engineering (OMAE)*, 2014. 59, 77

[93] M. Penalba, T. Kelly, and J. Ringwood, "Using NEMOH for Modelling Wave Energy Converters: A Comparative Study with WAMIT," in *Proceedings of the 12th European Wave and Tidal Energy Conference (EWTEC)*, (Cork, Ireland), p. 631, 2017. 63

[94] J. N. Newman and C. Lee, "WAMIT User Manual Version 7.0," tech. rep., Massachusetts Institute of Technology, Department of Ocean Engineering, 2013. 65

[95] J. Olondriz, I. Elorza, C. Calleja, J. Jugo, and A. Pujana, "Platform negative damping , blade root and tower base bending moment reductions with an advanced control technique," in *WindEurope Conference and Exhibition*, IOP Publishing, 2017. 71

[96] J. Olondriz, I. Elorza, J. Jugo, S. Alonso-Quesada, and A. Pujana-Arrese, "An Advanced Control Technique for Floating Offshore Wind Turbines Based on More Compact Barge Platforms," *Energies*, vol. 11, pp. 1187–1201, may 2018. xxvi, 71, 79, 82, 83, 85, 87

[97] R. Ramos, "Linear Quadratic Optimal Control of a Spar-Type Floating Offshore Wind Turbine in the Presence of Turbulent Wind and Different Sea States," *Journal of Marine Science and Engineering*, vol. 6, no. 4, p. 151, 2018. 72

[98] M. S. Khaniki, D. Schlipf, V. Pettas, and P. W. Cheng, "Control Design For Disturbance Rejection in Wind Turbines," in *Annual American Control Conference (ACC)*, IEEE, jun 2018. 72

[99] J. M. Jonkman, "Dynamics of offshore floating wind turbines-model development and verification," *Wind Energy*, vol. 12, pp. 459–492, 2009. 75

[100] J. M. Jonkman and M. L. Buhl, "Development and Verification of a Fully Coupled Simulator for Offshore Wind Turbines," in *45th AIAA Aerospace Sciences Meeting and Exhibit*, NREL/CP-500-40979, 2007. 75

[101] J. Jonkman and D. Matha, "Dynamics of Offshore Floating Wind Turbines-analysis of Three Concepts," *Wind Energy*, vol. 14, pp. 557–569, 2011. 79

[102] S. Christiansen, T. Bak, and T. Knudsen, "Damping Wind and Wave Loads on a FloatingWind Turbine," *Energies*, 2013. 83

[103] K. T. Magar and M. J. Balas, "Adaptive Individual Blade Pitch Control To Reduce Platform Pitch Motion Of A Floating Offshore Wind Turbine: Preliminary Study," in *Conference on Smart Materials, Adaptive Structures and Intelligent Systems SMASIS*, ASME, 2014. 83

[104] K. Kakita, N. Hara, and K. Konishi, "PI controller gain tuning with FRIT in collective blade pitch control of floating offshore wind turbines," in *15th International Conference on Control, Automation and Systems (ICCAS)*, IEEE, 2015. 83

[105] IEC 61400-3, "Wind Turbines - Part 3: Design Requirements for Offshore Wind Turbines," tech. rep., International Electrotechnical Commission (IEC), 2009. 90, 99

[106] IEC 61400-1 Ed. 3, "Wind Turbines - Part 1: Design Requirements," tech. rep., International Electrotechnical Commission (IEC), 2005. 90, 91

[107] J. M. Jonkman and D. Matha, "Dynamics of offshore floating wind turbines-analysis of three concepts," *Wind Energy*, vol. 14, pp. 557–569, 2011. 90, 99

[108] J. Jonkman, S. Butterfield, W. Musial, and G. Scott, "Definition of a 5-MW reference wind turbine for offshore system development," *Contract*, no. February, pp. 1–75, 2009. 94

[109] J. Olondriz, J. Jugo, I. Elorza, S. Alonso-Quesada, and A. Pujana-Arrese, "A Feedback Control Loop Optimisation Methodology for Floating Offshore Wind Turbines," *Energies (unpublished)*, 2019. 139

[110] M. Hall, B. Buckham, and C. Crawford, "Hydrodynamics-based floating wind turbine support platform optimization: A basis function approach," *Renewable Energy*, vol. 66, pp. 559–569, 2014. 140

[111] J. Gao and B. Sweetman, "Design optimization of hull size for spar-based floating offshore wind turbines," *Journal of Ocean Engineering and Marine Energy*, vol. 4, pp. 217–229, 2018. 140

[112] C. Scherer, P. Gahinet, and M. Chilali, "Multiobjective output-feedback control via LMI optimization," *IEEE Transactions on Automatic Control*, vol. 42, no. 7, pp. 896–911, 1997. 140

APPENDIX

A

Additional Data

A.1 Steady-State Operating Points

	NREL 5-MW ITI Energy			DTU 10-MW TripleSpar		
V_w (m/s)	Ω_r (rpm)	θ (deg)	θ_{yP} (deg)	Ω_r (rpm)	θ (deg)	θ_{yP} (deg)
11.4 - rated	12.1	0.00	2.01	9.6	0.00	2.72
12	12.1	3.83	1.56	9.6	4.61	2.10
13	12.1	6.52	1.39	9.6	7.44	1.78
14	12.1	8.70	1.19	9.6	9.50	1.58
15	12.1	10.40	1.14	9.6	11.24	1.45
16	12.1	12.06	1.00	9.6	12.79	1.33
17	12.1	13.49	0.98	9.6	14.22	1.25
18	12.1	14.92	0.88	9.6	15.56	1.17
19	12.1	16.18	0.85	9.6	16.82	1.11
20	12.1	17.47	0.79	9.6	18.03	1.06
21	12.1	18.67	0.76	9.6	19.19	1.02
22	12.1	19.94	0.71	9.6	20.31	0.98
23	12.1	21.18	0.68	9.6	21.40	0.95
24	12.1	22.35	0.61	9.6	22.45	0.92
25	12.1	23.37	0.58	9.6	23.47	0.89

Table A.1: Defined steady-state operating points for above rated wind speed.

APPENDIX

B

Simulink Schemes

B.1 Chirp Signal Simulink Scheme

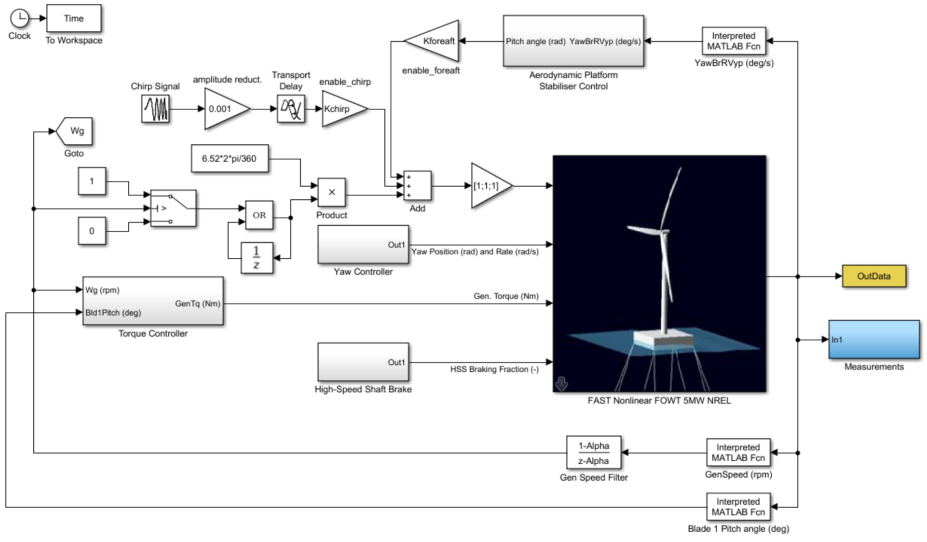

B.2 Control Simulink Scheme

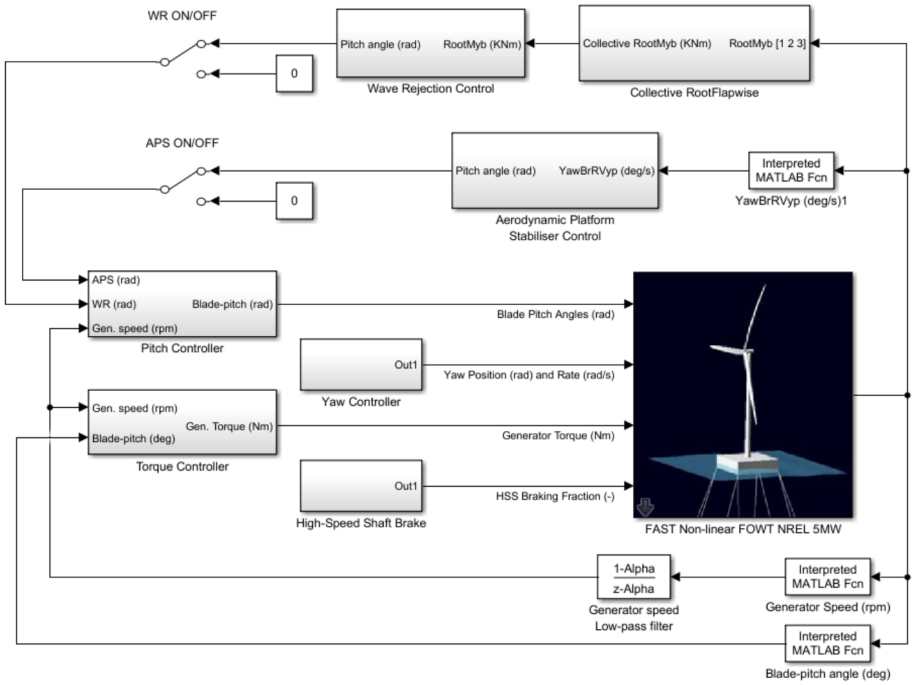

APPENDIX

C

Software Input Files

C.1 NEMOH Primary Input File

```
% Purpose : Create the main file for join up Mesh.m, Nemoh.m and
%           postNemoh.m files to generate from free floating bodies the
%           resulting hydrostatic forces and hydrodynamic coefficients as
%           the plots and figures requiered.
%
% Inputs : you have to decribe the platform faces and...
%     WaterDensity       : water density [Kg/m^3]
%     Gravity            : gravity acceleration [m/s^2]
%     A                  : platform total volume [m^3]
%     AR                 : aspect ratios
%     nBodies            : number of bodies to be meshed
%     n(nBodies)         : number of faces of the platform
%     X(nBodies,n,4,3)   : coordinates of nodes of each panel
%     tX(nBodies)        : translations
%     CG(nBodies,3)      : position of gravity centre
%     nfobj(nBodies)     : target number of panels for Aquaplus mesh
%     B                  : platform width
%     C                  : inner island width
%     D                  : plataform sumerged depth
%     w                  : wave periods
%     dir                : wave directions
%     depth              : sea depth
%
% Outputs : hydrostatics
%     KH.dat             : hydrostatic stiffness matrices file
%     CM.dat             : hydrodynamic added mass matrices file
%     CA.dat             : hydrodynamic damping coefficients matrices file
%
%


clear all
close all

savedir = pwd;                          % Save current directory (main folder)
```

C. SOFTWARE INPUT FILES

```
% Environmental conditions:
WaterDensity = 1025;                                % Water density [Kg/m^3]
Gravity = 9.81;                                     % Gravity acceleration [m/s^2]

% Platform physical
AR = [10 8 6 4 2 1];                                % Beam draught ratio
B = [40.23 35.71 30.98 25.86];                      % Plataform width
C = 10.0;                                           % Inner island width
D = [4.022 4.4639 5.1639 6.4647];                   % Plataform draught

A = B^2*D   C^2*D;                                  % Platform wetted volume [m^3]

for c = 1:length(AR)                                % Run NEMOH for each Aspect Ratio
        AR = AR(c);                                     % Select Aspect Ratio
        fprintf('Platform Aspect Ratio = %u',AR)        % Display current Aspect Ratio

        % Platform characteristics
        B = B(c);                                   % Current platform width
        D = D(c);                                   % Current platform depth

        % Platform description
        nBodies=1;                                                              % Number of bodies to mesh
        n=10;                                                                   % Number of platform faces
        X(1,1,:,:) = [B/2 0.0 0.0;B/2 0.0 D;B/2 B/2 D;B/2 B/2 0.0];             % Exterior face X
        X(1,2,:,:) = [B/2 B/2 0.0;B/2 B/2 D; B/2 B/2 D; B/2 B/2 0.0];           % Exterior face Y
        X(1,3,:,:) = [ B/2 0.0 0.0; B/2 B/2 0.0; B/2 B/2 D; B/2 0.0 D];         % Exterior face X
        X(1,4,:,:) = [B/2 0.0 D;C/2 0.0 D;C/2 B/2 D;B/2 B/2 D];                 % Bottom face 1
        X(1,5,:,:) = [C/2 C/2 D; C/2 C/2 D; C/2 B/2 D;C/2 B/2 D];               % Bottom face 2
        X(1,6,:,:) = [ C/2 0.0 D; B/2 0.0 D; B/2 B/2 D; C/2 B/2 D];             % Bottom face 3
        X(1,7,:,:) = [C/2 0.0 0.0;C/2 C/2 0.0;C/2 C/2 D;C/2 0.0 D];             % Exterior face X
        X(1,8,:,:) = [C/2 C/2 0.0; C/2 C/2 0.0; C/2 C/2 D;C/2 C/2 D];           % Exterior face Y
        X(1,9,:,:) = [ C/2 0.0 0.0; C/2 0.0 D; C/2 C/2 D; C/2 C/2 0.0];         % Exterior face X
        X(1,10,:,:)= [C/2 0.0 0.01; C/2 0.0 0.01; C/2 C/2 0.01;C/2 C/2 0.01];   % Face in Z
        tX(1)=0.0;                                                              % Translations
        CG(1,:) = [0.0 0.0 D/2];                                                % Floating center of the platform
        nfobj(1) = 3000;                                                        % Number of panels for the mesh

        % Hydrostatic calculation
        [HydrostaticStiffness] = Mesh(savedir,WaterDensity,Gravity,nBodies,n,X,tX,CG,nfobj);     % Lunch Mesh.m

        cd ([pwd,'\mesh']);             % Change directory from the main folder to mesh folder
        copyfile('mesh1.dat','../');    % Copy mesh1.dat file
        cd ('../');                     % Change directory returning to the main folder

        % Hydrodynamic data
        w = [0.05:0.05:5];              % Wave freq. [rad/s]
        dir = 0;                        % Wave direction [grad]
        depth = 0;                      % Water depth [m]

        % Hydrodynamic calculation
        [AddedMass,RadiationDamping] = Nemoh(w,dir,depth);          % Lunch Nemoh.m file

        % Data process
        postNemoh(WaterDensity,Gravity,A,B);                        % Lunch postNemoh.m file

        % Saving data files in folders
        cd (savedir);                                               % Return to main folder
        AR = int2str(AR);                                           % Change AR from number to string
        mallado = int2str(nfobj(1));                                % Change nfobj(1) from number to string
        fname = ['AspectRatio' AR '_' mallado];                     % Create the name of the folder
        mkdir('results',fname);                                     % Create the folder
        movefile('mesh/KH.dat',['results/' fname]);                 % Move KH.dat
        movefile('results/CA.dat',['results/' fname]);              % Move CA.dat
        movefile('results/CM.dat',['results/' fname]);              % Move CM.dat
end
```

C.2 HydroDyn Input File

```
        HydroDyn v2.03.* Input File
NREL 5.0 MW offshore baseline floating platform HydroDyn input properties for the ITI Barge with 4m draft.
False           Echo            Echo the input file data (flag)
                        ENVIRONMENTAL CONDITIONS
1025    WtrDens         Water density (kg/m^3)
150     WtrDpth         Water depth (meters)
0       MSL2SWL         Offset between still water level and mean sea level (meters) [positive upward; unused
                        WAVES
0       WaveMod         Incident wave kinematics model {0: none=still water, 1: regular (periodic), 1P#: regular
0       WaveStMod       Model for stretching incident wave kinematics to instantaneous free surface {0: none=no
3630    WaveTMax        Analysis time for incident wave calculations (sec) [unused when WaveMod=0; determines
0.25    WaveDT          Time step for incident wave calculations      (sec) [unused when WaveMod=0; 0.1<=WaveD
0       WaveHs          Significant wave height of incident waves (meters) [used only when WaveMod=1, 2, or 3]
"DEFAULT"       WavePkShp       Peak shape parameter of incident wave spectrum ( ) or DEFAULT (string) [used
0       WvLowCOff       Low  cut off frequency or lower frequency limit of the wave spectrum beyond which the
500     WvHiCOff        High cut off frequency or upper frequency limit of the wave spectrum beyond which the
0       WaveDir         Incident wave propagation heading direction                     (degrees) [unused
0       WaveDirMod      Directional spreading function {0: none, 1: COS2S}              ( )       [only used
1       WaveDirSpread   Wave direction spreading coefficient ( > 0 )                    ( )       [only used
1       WaveNDir        Number of wave directions                                       ( )       [only used
90      WaveDirRange    Range of wave directions (full range: WaveDir +/ 1/2*WaveDirRange) (degrees) [only used
123456789       WaveSeed(1)     First  random seed of incident waves [2147483648 to 2147483647]    ( )
1011121314  WaveSeed(2)     Second random seed of incident waves [2147483648 to 2147483647]    ( )
TRUE    WaveNDAmp       Flag for normally distributed amplitudes                        (flag)
""      WvKinFile       Root name of externally generated wave data file(s)       (quoted string)
1       NWaveElev       Number of points where the incident wave elevations can be computed ( )       [maximum of
0       WaveElevxi      List of xi coordinates for points where the incident wave elevations can be output
0       WaveElevyi      List of yi coordinates for points where the incident wave elevations can be output
                        2ND ORDER WAVES                                         [unused with WaveMod=0 or 6]
False   WvDiffQTF       Full difference frequency 2nd order wave kinematics (flag)
False   WvSumQTF        Full summation frequency  2nd order wave kinematics (flag)
0       WvLowCOffD      Low  frequency cutoff used in the difference frequencies (rad/s) [Only used with a
3.5     WvHiCOffD       High frequency cutoff used in the difference frequencies (rad/s) [Only used with
0.1     WvLowCOffS      Low  frequency cutoff used in the summation frequencies  (rad/s) [Only used with
3.5     WvHiCOffS       High frequency cutoff used in the summation frequencies  (rad/s) [Only used with
                        CURRENT                                                 [unused with WaveMod=6]
0       CurrMod         Current profile model {0: none=no current, 1: standard, 2: user defined from routine
0       CurrSSV0        Sub surface current velocity at still water level  (m/s) [used only when CurrMod=1]
"DEFAULT"       CurrSSDir       Sub surface current heading direction (degrees) or DEFAULT (string)
20      CurrNSRef       Near surface current reference depth            (meters) [used only when CurrMod=1]
0       CurrNSV0        Near surface current velocity at still water level (m/s) [used only when CurrMod=1]
0       CurrNSDir       Near surface current heading direction         (degrees) [used only when CurrMod=1]
0       CurrDIV         Depth independent current velocity                (m/s) [used only when CurrMod=1]
0       CurrDIDir       Depth independent current heading direction    (degrees) [used only when CurrMod=1]
                        FLOATING PLATFORM                                       [unused with WaveMod=6]
1       PotMod          Potential flow model {0: none=no potential flow, 1: frequency to time domain transforms
"HydroData\Barge"       PotFile         Root name of potential flow model data; WAMIT output files containing
1       WAMITULEN       Characteristic body length scale used to redimensionalize WAMIT output (meters) [only
6000    PtfmVol0        Displaced volume of water when the platform is in its undisplaced position (m^3)
0       PtfmCOBxt       The xt offset of the center of buoyancy (COB) from the platform reference point (meters)
0       PtfmCOByt       The yt offset of the center of buoyancy (COB) from the platform reference point (meters)
2       RdtnMod         Radiation memory effect model {0: no memory effect calculation, 1: convolution, 2: state
60      RdtnTMax        Analysis time for wave radiation kernel calculations (sec) [only used when PotMod=1;
0.0125  RdtnDT          Time step for wave radiation kernel calculations (sec) [only used when PotMod=1;
                        2ND ORDER FLOATING PLATFORM FORCES                      [unused with WaveMod=0 or 6,
0       MnDrift         Mean drift 2nd order forces computed                                  {0: None;
0       NewmanApp       Mean  and slow drift 2nd order forces computed with Newman's approximation {0: None;
0       DiffQTF         Full difference frequency 2nd order forces computed with full QTF     {0: None;
0       SumQTF          Full summation  frequency 2nd order forces computed with full QTF     {0: None;
                        FLOATING PLATFORM FORCE FLAGS                           [unused with WaveMod=6]
True    PtfmSgF         Platform horizontal surge translation force (flag) or DEFAULT
True    PtfmSwF         Platform horizontal sway translation force (flag) or DEFAULT
True    PtfmHvF         Platform vertical heave translation force (flag) or DEFAULT
True    PtfmRF          Platform roll tilt rotation force (flag) or DEFAULT
True    PtfmPF          Platform pitch tilt rotation force (flag) or DEFAULT
True    PtfmYF          Platform yaw rotation force (flag) or DEFAULT
```

```
                    PLATFORM ADDITIONAL STIFFNESS AND DAMPING
* all zeros
                    AXIAL COEFFICIENTS
1       NAxCoef         Number of axial coefficients ( )
AxCoefID  AxCd      AxCa      AxCp
( )     ( )       ( )       ( )
1       0.00      0.00      1.00
                    MEMBER JOINTS
2       NJoints         Number of joints ( )   [must be exactly 0 or at least 2]
JointID   Jointxi     Jointyi     Jointzi   JointAxID   JointOvrlp   [JointOvrlp= 0: do nothing at joint,
( )       (m)         (m)         (m)       ( )         (switch)
1       0.00000     0.00000     4.00000     1           0
2       0.00000     0.00000     0.00000     1           0
                    MEMBER CROSS SECTION PROPERTIES
1       NPropSets       Number of member property sets ( )
PropSetID   PropD        PropThck
( )         (m)         (m)
1       45.13520        0.00010
                    SIMPLE HYDRODYNAMIC COEFFICIENTS (model 1)
SimplCd   SimplCdMG   SimplCa   SimplCaMG   SimplCp   SimplCpMG   SimplAxCa   SimplAxCaMG   SimplAxCp
( )       ( )         ( )       ( )         ( )       ( )         ( )         ( )           ( )
1.00      1.00        0.00      0.00        1.00      1.00        1.00        1.00          1.00
                    DEPTH BASED HYDRODYNAMIC COEFFICIENTS (model 2)
0       NCoefDpth       Number of depth dependent coefficients ( )
Dpth      DpthCd    DpthCdMG    DpthCa    DpthCaMG      DpthCp    DpthCpMG    DpthAxCa    DpthAxCaMG
(m)       ( )       ( )         ( )       ( )           ( )       ( )         ( )         ( )
                    MEMBER BASED HYDRODYNAMIC COEFFICIENTS (model 3)
0       NCoefMembers        Number of member based coefficients ( )
MemberID  MemberCd1   MemberCd2   MemberCdMG1   MemberCdMG2   MemberCa1   MemberCa2   MemberCaMG1   MemberCaMG2
MemberCp1   MemberCp2   MemberCpMG1   MemberCpMG2   MemberAxCa1   MemberAxCa2
( )       ( )         ( )         ( )           ( )           ( )         ( )         ( )
( )         ( )           ( )           ( )           ( )           ( )         ( )           ( )
                    MEMBERS
1       NMembers        Number of members ( )
MemberID  MJointID1   MJointID2   MPropSetID1   MPropSetID2   MDivSize    MCoefMod    PropPot    [MCoefMod=1: use
( )       ( )         ( )         ( )           ( )           (m)         (switch)    (flag)
1         1           2           1             1             0.5000      1           TRUE
                    FILLED MEMBERS
0       NFillGroups     Number of filled member groups ( ) [If FillDens = DEFAULT, then FillDens = WtrDens;
FillNumM  FillMList           FillFSLoc     FillDens
( )       ( )                 (m)           (kg/m^3)
                    MARINE GROWTH
0       NMGDepths       Number of marine growth depths specified ( )
MGDpth    MGThck      MGDens
(m)       (m)         (kg/m^3)
                    MEMBER OUTPUT LIST
0       NMOutputs       Number of member outputs ( ) [must be < 10]
MemberID        NOutLoc     NodeLocs [NOutLoc < 10; node locations are normalized distance from the start of
( )       ( )       ( )
                    JOINT OUTPUT LIST
0       NJOutputs       Number of joint outputs [Must be < 10]
0       JOutLst         List of JointIDs which are to be output ( )[unused if NJOutputs=0]
                    OUTPUT
True    HDSum           Output a summary file [flag]
False   OutAll          Output all user specified member and joint loads (only at each member
2       OutSwtch        Output requested channels to: [1=Hydrodyn.out, 2=GlueCode.out, 3=both files]
"ES11.4e2"      OutFmt          Output format for numerical results (quoted string) [not checked for
"A11"   OutSFmt         Output format for header strings (quoted string) [not checked for
                    OUTPUT CHANNELS
"Wave1Elev"         Wave elevation at the platform reference point (0,0), (m)
END of output channels and end of file. (the word "END" must appear in the first 3 columns of this line)

END of output channels and end of file. (the word "END" must appear in the first 3 columns of this line)
"TTDspSS"                   Tower top/yaw bearing side to side (translational) deflection (relative
END of input file (the word "END" must appear in the first 3 columns of this last OutList line)
```

APPENDIX

D

Simulation Results

D.1 Manually Tuned Controller Performance Extreme-Events

Parameter	Controller	Type	Conditions	Value (KNm)	Time (sec)
M_{yT} (TwrBsMyt)	Detuned PI	Min	V_w = 25m/s H_s = 6m	-5,431E+05	3172,2
		Max	V_w = 21m/s H_s = 6m	4,682E+05	2767,2
	Detuned PI & APS	Min	V_w = 15m/s H_s = 6m	-4,338E+05	497,0
		Max	V_w = 13m/s H_s = 6m	4,772E+05	2767,1
	Detuned PI & APS & WR	Min	V_w = 25m/s H_s = 6m	-5,063E+05	3171,9
		Max	V_w = 13m/s H_s = 6m	4,806E+05	2767,2
M_{xT} (TwrBsMxt)	Detuned PI	Min	V_w = 25m/s H_s = 6m	-1,440E+05	598,6
		Max	V_w = 25m/s H_s = 6m	1,699E+05	1880,0
	Detuned PI & APS	Min	V_w = 23m/s H_s = 6m	-1,253E+05	3252,2
		Max	V_w = 23m/s H_s = 6m	1,566E+05	3257,9
	Detuned PI & APS & WR	Min	V_w = 25m/s H_s = 6m	-1,670E+05	2304,0
		Max	V_w = 25m/s H_s = 6m	1,841E+05	1878,5

Parameter	Controller	Type	Conditions	Value (KNm)	Time (sec)
M_{yB} (RootMyb1)	Detuned PI	Min	V_w = 25m/s H_s = 6m	-1,702E+04	498,8
		Max	V_w = 25m/s H_s = 6m	2,349E+04	506,6
	Detuned PI & APS	Min	V_w = 25m/s H_s = 6m	-2,077E+04	2354,0
		Max	V_w = 25m/s H_s = 6m	2,438E+04	2351,0
	Detuned PI & APS & WR	Min	V_w = 25m/s H_s = 6m	-1,910E+04	498,7
		Max	V_w = 13m/s H_s = 6m	2,089E+04	326,2
M_{xB} (RootMxb1)	Detuned PI	Min	V_w = 21m/s H_s = 6m	-9,700E+03	1853,3
		Max	V_w = 23m/s H_s = 6m	1,037E+04	1782,9
	Detuned PI & APS	Min	V_w = 23m/s H_s = 6m	-9,511E+03	1877,4
		Max	V_w = 21m/s H_s = 6m	1,016E+04	3172,6
	Detuned PI & APS & WR	Min	V_w = 25m/s H_s = 6m	-9,159E+03	2305,0
		Max	V_w = 23m/s H_s = 6m	8,747E+03	2674,8

D.2 Optimised Controller Performance Extreme-Events

Parameter	Controller	Type	Conditions	Value (KNm)	Time (sec)
M_{yT} (TwrBsMyt)	Detuned PI	Min	V_w = 25m/s H_s = 6m	-5,431E+05	3172,2
		Max	V_w = 21m/s H_s = 6m	4,682E+05	2767,2
	Manually APS & WR	Min	V_w = 25m/s H_s = 6m	-5,063E+05	3171,9
		Max	V_w = 13m/s H_s = 6m	4,806E+05	2767,2
	Optimised APS & WR	Min	V_w = 19m/s H_s = 6m	-4,816E+05	3172,1
		Max	V_w = 25m/s H_s = 6m	4,793E+05	2767,1
M_{xT} (TwrBsMxt)	Detuned PI	Min	V_w = 25m/s H_s = 6m	-1,440E+05	598,6
		Max	V_w = 25m/s H_s = 6m	1,699E+05	1880,0
	Manually APS & WR	Min	V_w = 25m/s H_s = 6m	-1,670E+05	2304,0
		Max	V_w = 25m/s H_s = 6m	1,841E+05	1878,5
	Optimised APS & WR	Min	V_w = 23m/s H_s = 6m	-1,434E+05	2303,9
		Max	V_w = 25m/s H_s = 6m	1,411E+05	1610,8
M_{yB} (RootMyb1)	Detuned PI	Min	V_w = 25m/s H_s = 6m	-1,702E+04	498,8
		Max	V_w = 25m/s H_s = 6m	2,349E+04	506,6
	Manually APS & WR	Min	V_w = 25m/s H_s = 6m	-1,910E+04	498,7
		Max	V_w = 13m/s H_s = 6m	2,089E+04	326,2
	Optimised APS & WR	Min	V_w = 23m/s H_s = 6m	-2,003E+04	498,5
		Max	V_w = 19m/s H_s = 6m	2,099E+04	326,1
M_{xB} (RootMxb1)	Detuned PI	Min	V_w = 21m/s H_s = 6m	-9,700E+03	1853,3
		Max	V_w = 23m/s H_s = 6m	1,037E+04	1782,9
	Manually APS & WR	Min	V_w = 25m/s H_s = 6m	-9,159E+03	2305,0
		Max	V_w = 23m/s H_s = 6m	8,747E+03	2674,8
	Optimised APS & WR	Min	V_w = 25m/s H_s = 6m	-1,004E+04	1853,2
		Max	V_w = 25m/s H_s = 6m	9,080E+03	496,0

D.3 Time-Domain Simulations NREL 5-MW Beam-Draught Ratio 6 Barge

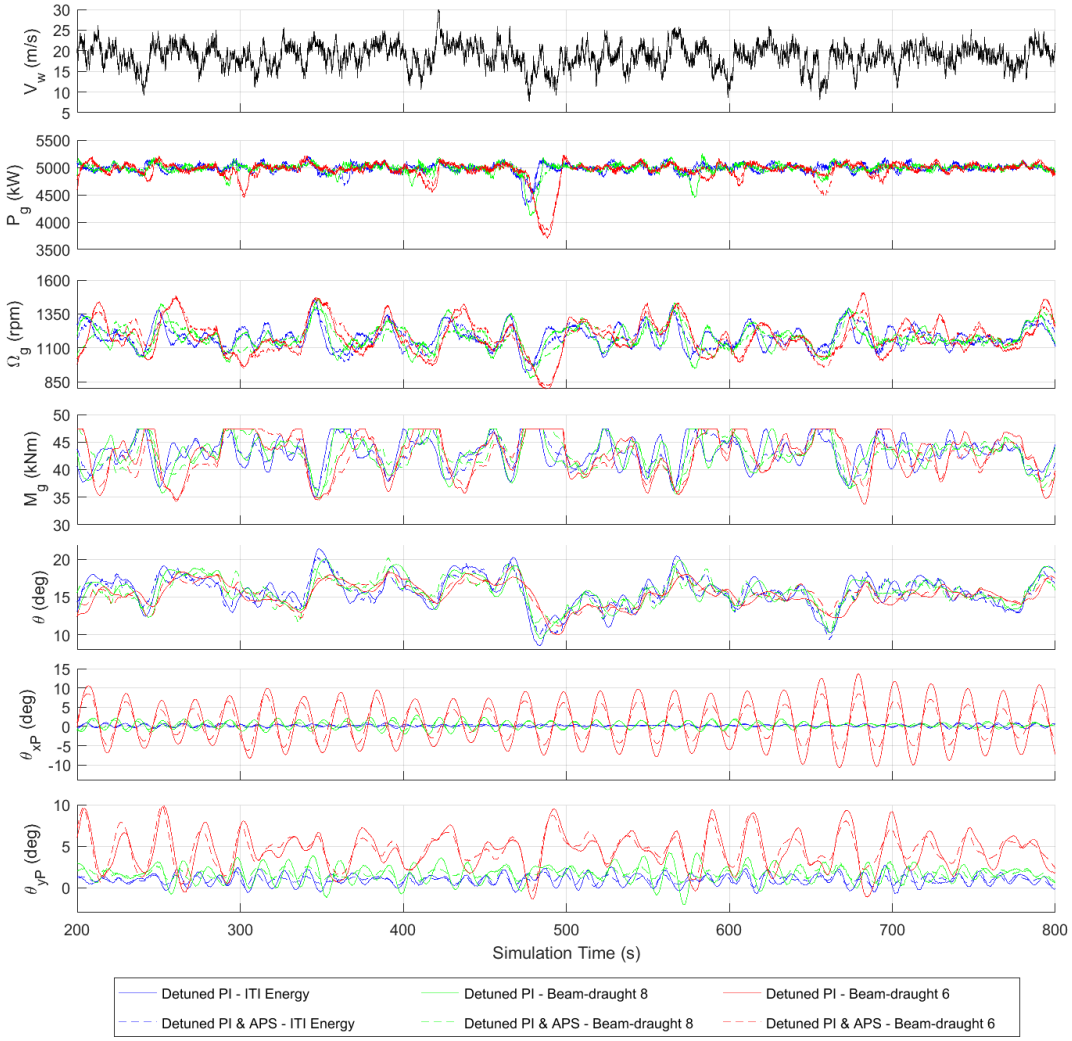

Declaration

I herewith declare that I have produced this work without the prohibited assistance of third parties and without making use of aids other than those specified; notions taken over directly or indirectly from other sources have been identified as such. This work has not previously been presented in identical or similar form to any examination board. Except where indicated by specific reference in the text, the work is the candidate's own work. Work done in collaboration with, or with the assistance of, others, is indicated as such. Any views expressed in the dissertation are those of the author.

This dissertation was finished in Leioa, 2019.

This page is intentionally left blank